The Journal of Chemical Physics

Understanding noncovalent bonds and their controlling forces

Cite as: J. Chem. Phys. **153**, 140901 (2020); https://doi.org/10.1063/5.0026168
Submitted: 21 August 2020 • Accepted: 15 September 2020 • Published Online: 09 October 2020

Steve Scheiner

The Journal of Chemical Physics PERSPECTIVE scitation.org/journal/jcp

Understanding noncovalent bonds and their controlling forces

Cite as: J. Chem. Phys. 153, 140901 (2020); doi: 10.1063/5.0026168
Submitted: 21 August 2020 • Accepted: 15 September 2020 •
Published Online: 9 October 2020

Steve Scheiner[a]

AFFILIATIONS

Department of Chemistry and Biochemistry, Utah State University, Logan, Utah 84322-0300, USA

[a]Author to whom correspondence should be addressed: steve.scheiner@usu.edu

ABSTRACT

The fundamental underpinnings of noncovalent bonds are presented, focusing on the σ-hole interactions that are closely related to the H-bond. Different means of assessing their strength and the factors that control it are discussed. The establishment of a noncovalent bond is monitored as the two subunits are brought together, allowing the electrostatic, charge redistribution, and other effects to slowly take hold. Methods are discussed that permit prediction as to which site an approaching nucleophile will be drawn, and the maximum number of bonds around a central atom in its normal or hypervalent states is assessed. The manner in which a pair of anions can be held together despite an overall Coulombic repulsion is explained. The possibility that first-row atoms can participate in such bonds is discussed, along with the introduction of a tetrel analog of the dihydrogen bond.

I. INTRODUCTION

The term "noncovalent bond" refers to almost any interaction that is weaker than a covalent bond, which covers a lot of territory. Using the strength of the interaction as a measure, the very weak end of this spectrum might involve, for example, the interaction between rare gas atoms, such as He_2 or Ar_2, or between highly nonpolar molecules such as alkanes. As a numerical example, the interaction energy between methanol and a rare gas atom lies in the range of 0.07 kcal/mol–0.44 kcal/mol,[1] rising in value along with the size of the particular rare gas atom, and is composed largely of dispersion energy. The argon dimer itself[2] is bound by only 0.3 kcal/mol, composed almost exclusively of dispersion. On the opposite end of this spectrum are the very strong interactions such as ionic bonds between ions of opposite charge, as in $K^+\cdots Cl^-$, isoelectronic with Ar_2, on the order of 100 kcal/mol–200 kcal/mol or even more if the ions bear a multiple charge. While each of these extremes is of some interest and continues to engender research into various facets of their nature, their natures are largely understood in that two spherically symmetric Ar atoms are held together by weak London dispersion forces, and the driving attractive force in an ion pair is a Coulombic attraction, which is coupled with polarization phenomena.

Most of the current interest in noncovalent bonds is centered around those lying near the middle of this spectrum, of moderate strength, on the order of perhaps 3 kcal/mol–20 kcal/mol. There are a great many interactions that fall into this range. The stacking interactions between aromatic systems are a prime example,[3–6] an essential force in the stability of DNA in the guise of parallel pairs of nucleic acid dimers. The placement of an ion above an aromatic system leads to ion-π interactions that have engendered a good deal of study as well. The n → π* interactions between C=O groups fall within this range as well, with interaction energies in this range.[7–19]

Almost certainly, the best known and thoroughly studied noncovalent interaction is the H-bond.[20–28] A century of examination has led to a solid understanding of this bond, its underlying nature, and the separate physical phenomena that contribute to its stability, as well as the experimental manifestations of its presence. However, there are a number of close cousins of the H-bond whose existence and properties remain largely unappreciated. As will be described below, their very existence as a stabilizing force seems counterintuitive at first glance, since they seem to defy common understandings of atomic electronegativity. However, they are very much a fact, and the rapidly growing recognition of their properties is leading to major advances in several fields of chemistry and biology. This Perspective article represents an attempt to introduce these noncovalent

bonds to a reader that might be unfamiliar with them, to explain their underlying nature, and to examine their properties.

II. ENERGETIC MEASURES OF STRENGTH

Although noncovalent bonds such as the H-bond (HB) are commonly referred to as strong or weak, it is necessary to come to some common understanding of the meaning of this qualifier. Can we quantify this concept of bond strength? Just as the strength of a covalent bond represents the energy required to dissociate this bond, so too can the dissociation of a noncovalent bond into its constituent monomers be taken as the bond strength. This quantity is usually defined as the energy of association reaction (1), ΔE, or as it is commonly referred to in the literature as the binding energy E_b,

$$A + B \rightarrow A\cdots B. \quad (1)$$

Note that ΔE will be negative for this association reaction, and its magnitude can be used as a simple and universal gauge of the noncovalent bond strength. There are several potentially complicating issues with this metric in the context of quantum calculations. ΔE is usually presented as the difference in purely electronic energies of products vs reactants. Conversion into ΔH requires the addition of other terms, chief among them being the vibrational energies. Further extrapolation into Gibbs free energy is achieved through entropic effects.

A closely associated metric of noncovalent bond energy is the interaction energy E_{int}. This quantity is very much like ΔE in Eq. (1) except that the energies of the A and B constituents are not taken in their isolated optimized geometries but rather in the geometries they adopt within the optimized A···B complex. E_{int} might thus be thought of as a purer measure of the actual interaction occurring within this complex, once the monomers have adjusted their geometries. E_{int} differs from E_b by E_{def}, the energy required to deform each optimized monomer into its structure within the complex. In many, but not all, cases of noncovalent bond formation, these two geometries are not very different, E_{def} is fairly small, and E_{int} is thus roughly equal to E_b. However, the reader should be wary of those interactions that require substantial monomer rearrangements, some of which will be outlined below.

There are a host of noncovalent interactions that occur that are not between two fully separate entities but rather within a single molecular unit. An example might be the HBs within a single α-helix of a protein or an intramolecular HB in a system such as malonaldehyde. Since A and B in Eq. (1) refer to different molecules, this equation can no longer be employed, and thus, ΔE is undefined. However, despite this obstacle, it is clear that some internal HBs are stronger than others, so surely there must be some metric for this situation as well. More will be said about this issue later, but for the time being, it is sufficient that the reader be apprised of this potential difficulty and be wary of papers in the literature that purport to calculate intramolecular noncovalent bond energies as such evaluations always involve a certain degree of arbitrariness or of arguable equations.[29–34]

As this discourse concerns itself with noncovalent bonds, the obvious question arises as to how to know one when you see it. The concept of bond energy offers one means of making this distinction. Since covalent bonds are typically on the order of 100 kcal/mol or more and most noncovalent bonds are less than about 30 kcal/mol, the difference between the two would seem obvious. Unfortunately, things are not always so simple. There are a number of different interactions with bond energies in the standard noncovalent range, but with appropriate gradual modifications of substituents, for example, they can advance into the energy range normally reserved for covalent bonds. On this basis, as well as others to be described in more detail below, it must be understood that the borderline between the two designations can be a murky one.

A. Components of H-bond energy

Given the similarities between the new set of noncovalent bonds to be described below and the H-bond, it would be useful to first review the principles concerning the latter. A HB is established between an AH acid and a base B wherein the H acts as a bridge between the two subunits: AH···B. There are several phenomena that contribute to this interaction. In the first place, the A to which the H is attached is typically rather electronegative so that the acid is polarized $^{-}A—H^{+}$ with a positive H end. The base is oriented so that its own partial negative charge approaches the H of the acid, culminating in an electrostatic attraction. Of course, this H···B atom-to-atom picture of the electrostatic interaction is a gross oversimplification. One can take a step closer to the complete picture by considering the interactions between the dipole moments of the two subunits. Or it is better yet to enlarge consideration to higher orders of the multipole moments, e.g., quadrupoles and octapoles. However, even that treatment is only approximate and breaks down as the two subunits come closer together. The full electrostatic component involves a complete treatment of all interactions between nuclei, electrons, and the nucleus and electron.

However, this Coulombic force is only part of the story. Along the lines of the old idea of a charge-transfer complex, a certain amount of charge is transferred from the base B, usually from its lone pair, into the σ^*(AH) antibonding orbital of the acid. In addition to the energetic stabilization accruing from this transfer, there is also a weakening of the A—H covalent bond. It is this latter phenomenon that accounts for the well-known red shift of the A—H stretching frequency, as well as its elongation. Besides this particular interorbital transfer, there are other transfers between the two molecules, in addition to shifts of electron density within each subunit that are caused by the perturbing approach of the other molecule. All of these redistributions of electron density fall under various rubrics such as charge transfer, polarization, orbital interactions, and induction.

For a typical HB, the electrostatic component accounts for a bit more than half of the total interaction energy. The induction term is a bit smaller, but its omission would introduce a large error into the treatment. Even smaller, but again not negligible, is the London dispersion attraction. This quantity usually enlarges as larger and more polarizable atoms are introduced into the system.

III. REPLACEMENT OF BRIDGING PROTON

Now, let us consider the situation where the bridging H atom of the acid is replaced by another atom. As an extreme variation, we will replace H with a highly electronegative halogen X atom. The first and intuitive response would be that the electronegative X atom should

lead to the reverse polarization of the AX molecule to $^{+}A-X^{-}$, and X would then repel any nucleophile. While there is some superficial validity to this objection, it is not the whole story. While the net charge on the X atom might certainly be partially negative, it is not uniformly negative. That is, the charge distribution around the X atom is quite anisotropic; it has been described as a "polar flattening"[35–41] as charge is drawn in toward the A—X covalent bond, leaving a deficit along the pole, i.e., the extension of the A—X bond axis. So, the total electrostatic potential contains a negative belt around the X equator, along with a positive polar region along the extension of that bond, commonly referred to as a σ-hole.[42,43] In other words, even an atom as electronegative as a halogen atom has a positive region attached to it. In addition, it is this positive area that can attract a nucleophile in exactly the same way as the positively charged H of AH in a HB.

The second major contributing factor to a HB is the charge donation from the base to the σ^*(AH) antibonding orbital. Well, there is such an orbital present as well within the Lewis acid molecule after H has been replaced by X. The accumulation of charge in the σ^*(AX) orbital ought to similarly weaken and stretch this covalent bond. Nor should the dispersion contribution to H-bonding be any less applicable following the replacement of the H. Indeed, the larger X atom with its greater number of electrons and more polarizable nature ought to be subject to even larger dispersion forces.

The reader may have surmised that there is nothing special about the halogen family that leads to this phenomenon of a σ-hole. In fact, the same is true of other families, viz., the S, Se chalcogen series, as well as the pnicogen (P, As) and tetrel (Si, Ge) families. This phenomenon is also characteristic of others such as the triels (B, Al) and even the inert gas atoms (aerogens) when involved in a bonding situation within a molecule.[44,45] It should also be considered that as the halogens are the most electronegative of these sets of families, one might expect the positive σ-holes to be even more intense on some of these other less electronegative atoms.

Given these ideas, it ought not be surprising that any of these replacements will lead to an interaction that is fully consistent with and similar to the HB. While this entire set of interactions can be classified as σ-hole bonds, it is more common to use subclassifications depending on the particular family from which the bridging atom is drawn. Hence, the incorporation of a halogen atom such as Cl or Br is commonly termed a halogen bond (XB), with an obvious parallel nomenclature for a chalcogen bond (YB), pnicogen bond (ZB), tetrel bond (TB), triel bond (TrB), and aerogen bond (AeB) (alternately called the noble gas bond, NgB). The bulk of this Perspective describes the most important aspects of these bonds.

While the total literature concerning the XB is probably the most extensive and goes back furthest in time,[38,46–60] work on the YB,[61–73] ZB,[74–78] TB,[79–83] TrB,[84–88] and AeB[45,89–92] is also progressing nicely at this point in time, and our understanding of these interactions continues to grow at a rapid pace.

A. Controlling factors and general rules

There are a number of factors that are common to these various σ-hole bonds.

As one moves down a column of the periodic table, the elements become more electropositive and more polarizable. Both of these factors lead to the intensification of the σ-hole, greater ability to accept electron density from the Lewis base, and a higher amount of attractive dispersion. So, these bonds become stronger as the bridging atom drops down in the periodic table. Indeed, it is questionable whether the first-row atoms such as F and N can participate in such bonds at all, at least under normal circumstances.

Electron-withdrawing substituents on the Lewis acid molecule will draw density away from the bridging atom and intensify the σ-hole. These substituents will also facilitate the Lewis acid's ability to acquire charge from the base, so the bond will strengthen. Electron-releasing substituents on the base will also strengthen the bond for parallel reasons.

Placement of a positive charge on the Lewis acid and/or a negative charge on the base will enhance these bonds in the same way that a charge can assist the stabilization of HBs.

There is no widely applicable rule as to the comparative strengths of XB, YB, ZB, or TB, at least in the general sense.

Because of the normal tetravalent bonding character of tetrel (T) atoms, each of their four σ-holes, opposite to a R—T covalent bond, suffers from reduced accessibility due to steric crowding from the neighboring R substituents. The formation of a TB, therefore, requires these crowding substituents to move out of the way to some degree and so typically involves a substantial degree of monomer deformation.

Due to the charge transferred into the σ^*(R—A) antibonding orbital (where A represents the generic bridging atom and R represents a substituent), the RA bond generally lengthens and weakens, with an associated red shift of its stretching frequency. However, this is not always the case, in the same way that certain HBs defy the general rule and shift to the blue.[93–100]

The formation of a HB reduces the electron density surrounding the bridging proton and its attendant shielding, causing its nuclear magnetic resonance (NMR) signal to shift downfield. The opposite effect of increased shielding seems to be characteristic of the other σ-hole bonds.

Although the donor orbital on the base is typically a lone pair, this same function can be served by π-systems,[101–104] whether aromatic or non-aromatic, and in rarer circumstances by σ-bonds[105–111] or occupied d-orbitals[112–116] of a metal atom.

All of these bonds, whether H-bonding or one of its related counterparts, are subject to cooperativity effects when more than one is present. The bonds strengthen one another if the central unit acts simultaneously as both the electron donor and acceptor, while the opposite effect of mutual weakening occurs in the case of double-donor or double-acceptor.

IV. DEVELOPMENT OF A NONCOVALENT BOND

It serves an instructional purpose to watch as one of these bonds begins to form. In order to do so, one can take the two subunits at some distance apart and then gradually allow them to approach one another, monitoring the physical attributes of the system as we do so.

A. Coulombic forces

We begin the process at a long distance, at which point it is only the electrostatic interaction that reaches out this far. We will take as

our prototype system the halogen bond in $F_3CBr\cdots NH_3$. The three F atoms on the acid ought to intensify the σ-hole on the bridging Br atom, and the lone pair of NH_3 serves as a typical example of an electron donor. Since both units are neutral, there is no charge–charge component to the electrostatic interaction. The highest nonzero element of the multipole expansion would be dipole–dipole. The dipole moments of F_3CBr and NH_3 are calculated to be 0.655 D and 1.801 D, respectively, so the dipole–dipole interaction would be equal to $-17.0/R^3$ kcal/mol, where R is expressed in Å.

The (μ–μ) dipole–dipole interaction is illustrated in Fig. 1 as the red curve, which undergoes only a gradual increase in the absolute value as the two monomers approach one another, remaining below 0.5 kcal/mol even for an intermolecular distance as short as 4 Å. The full electrostatic component is of course a much more complete treatment of the interactions between the entire electronic and nuclear dispositions of the two subunits and includes the dipole–dipole term implicitly as one of its many elements. The total ES interaction energy is indicated by the black curve in Fig. 1. Although it is comparable to the μ–μ interaction for very long distances, the full ES term quickly diverges and becomes much more negative, even for intermolecular distances as long as 8 Å. It is clear then that while the dipole orientations might provide clues as to the optimal orientations of the two molecules, they are of little value in estimating the actual magnitude of the electrostatic attraction.

As the two subunits approach one another more closely than about 8 Å, the shorter-range components of the interaction, such as induction and dispersion, begin to kick in. The full quantum mechanical interaction energy in blue is thus much more negative than the red electrostatic ES curve for progressively smaller R. With a much stronger sensitivity to R than ES, both induction and dispersion quickly become prominent players as R continues to decrease.

Since ES is not a good quantitative measure of the full interaction energy, does it offer some particular value in its own right? In essence, the answer is strongly affirmative. The ES component is highly anisotropic. So, the optimal use of the electrostatic potential surrounding each molecule is to act as a guide as to how the two molecules will orient as they approach one another. Taking the $F_3CBr\cdots NH_3$ complex as an example again, the molecular electrostatic potential (MEP) of each of the two individual monomers is diagrammed in Fig. 2, where red and blue refer to negative and

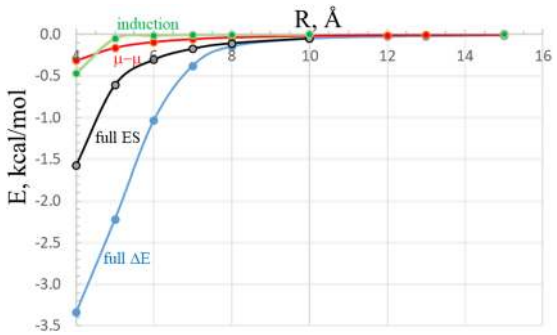

FIG. 1. Behavior of various energetic properties of the $F_3CBr\cdots NH_3$ system in terms of intermolecular R(Br···N) distance.

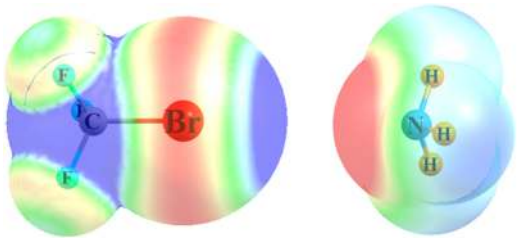

FIG. 2. Molecular electrostatic potentials surrounding F_3CBr and NH_3 monomers. Red and blue regions refer, respectively, to negative and positive potentials.

positive regions, respectively. The σ-hole along the extension of the C—Br bond is laid out in the corresponding blue segment, and the negative MEP that coincides with the N lone pair of NH_3 is represented by its red area. It is therefore sensible that the two molecules will attract one another best when they are in the orientation consistent with a linear C—Br···N halogen-bonding arrangement. Of course, each molecule contains other red and blue regions. So, the XB structure is not the only one that aligns red with blue. For example, it is conceivable that the positive blue areas around the NH_3 protons might favorably approach the red region around the equatorial belt of the Br atom of F_3CBr so as to engage in a NH···Br H-bond. Another possibility would entail the N lone pair approaching the positive blue area near the C atom of F_3CBr, which might constitute a FC···N tetrel bond. However, even though both sections are blue, a more quantitative assessment places the positive region near the Br as more positive than that near the C (see below). Moreover, there are actually two sorts of blue regions near the C atom, those opposite F atoms and that opposite the Br atom, both of which are less positive than that near the Br atom. It is the primary function of inspection of the MEP of each molecule to lay out a number of candidate geometries, but it is up to full quantum calculations to rank order these structures in terms of energy.

The MEP surrounding a given molecule is a three-dimensional function, so there are questions concerning the best way to illustrate it in an easily digestible manner. For example, the MEPs in Fig. 2 each represent its value on a surface that represents 1.5× the vdW radius of each atom. The value of the MEP is color-coded, from red to blue. However, the actual values taken for the extremes are chosen so as to highlight the most important aspects. For NH_3, for example, these extremes were chosen as ±0.005 a.u., while they were +0.020 a.u. and −0.001 a.u. for F_3CBr. Using the same extrema for the two molecules would obscure their most important aspects for purposes of their interactions with one another. Of course, other surfaces are quite reasonable as well. The sensitivity of the MEP to the distance of each surface from the various nuclei is exhibited in Fig. 3. Because the contraction of the surface from twice to 1.5 to 1.0 times the vdW radius brings one in closer to the nuclei and below the shielding of some of the electron cloud, the MEP becomes progressively more positive, as reflected in the scales associated with each diagram. However, the important features remain in all three, viz., a σ-hole along the C—Br extension and a negative equatorial belt around the Br atom.

It is possible to take these ideas and make them a bit more quantitative. That is, one can compute the value of the MEP at the σ-hole

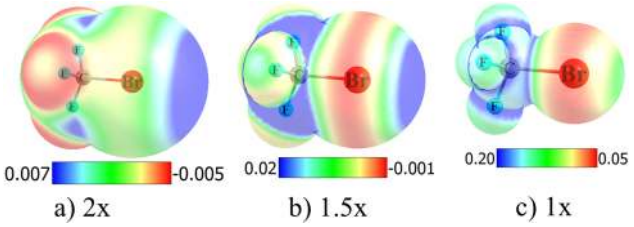

FIG. 3. Molecular electrostatic potentials (a.u.) surrounding F_3CBr on surfaces corresponding to different multiples of the vdW radius of each atom.

TABLE I. Values of MEP maxima (kcal/mol) on various isodensity surfaces of F_3CBr.

ρ (a.u.)	0.000 01	0.0001	0.001	0.005
R[a] (Å)	3.12	2.61	2.03	1.63
Br_C	7.8	12.5	26.2	55.5
C_{Br}	...	5.4	20.8	55.1
C_F	0.6	3.9	16.3	50.0
F_C	...	−2.1	−1.3	4.4

[a]Distance from Br to Br_C maximum.

on the Br atom and assign it a numerical value. However, in order to do so, there must be some understanding as to where exactly this point ought to be. Of course, along the C—Br axis, but where exactly along this line? The most commonly accepted practice has been to compute the MEP on an isodensity surface, usually taken as ρ = 0.001 a.u., and locate the maximum of the MEP on this particular surface. This quantity is typically designated as $V_{s,max}$ in the literature. In the example of F_3CBr, there are in fact several maxima on the surface, as indicated in Fig. 4. The σ-hole maximum along the extension of the C—Br axis, denoted Br_C, is the most intense of these with $V_{s,max}$ = 26.2 kcal/mol, as reported in Table I. Another C_{Br} σ-hole occurs on the opposite end of the Br—C axis, near the C atom, with a slightly lower value of 20.8 kcal/mol. There are other σ-holes along the F—C axis near the C atom, C_F, that are still less intense at 16.3 kcal/mol. Finally, there are also σ-holes near the F atoms along the C—F axes, F_C, albeit with slightly negative $V_{s,max}$ = −1.3 kcal/mol. So, one might take these relative values as a guide that the Br_C hole is the strongest and so ought to best attract the NH_3 to form a CBr···N XB. However, a BrC···N tetrel bond must be considered as well as this σ-hole is only slightly less intense, with a FC···N tetrel bond also on the list of candidates to be tested.

However, on the other hand, the choice of ρ = 0.001 is only one of many possibilities. Suppose another density were chosen, 0.0001 a.u., for example, which would move the maxima further away from the various atoms and perhaps closer to where the electrostatic interaction is more important. As indicated in Table I, the Br_C point moves from 2.03 Å away from Br when ρ = 0.001 a.u. to 2.61 Å. Doing so retains all of these maxima in the MEP, and they retain their orientations, changing only their distances from the atoms. On a quantitative level, the lowered density reduces the values of all of the $V_{s,max}$ since these positions are all further from the nuclei. The primary hole near Br drops from 26.2 kcal/mol to 12.5 kcal/mol, and the others are also reduced to 5.4, kcal/mol 3.9 kcal/mol, and −2.1 kcal/mol, respectively. However, importantly, all of these σ-holes remain in place at the reduced density and retain their relative ordering. Still, another step away from the molecule may be taken with the choice of ρ = 0.000 01 a.u. The MEP maximum corresponding to the Br_C σ-hole is now located some 3.12 Å from the Br atom. This further removal from the nuclei again lowers $V_{s,max}$ to 7.8 kcal/mol, and the C_F maxima drop to 0.6 kcal/mol. However, there is no longer a single maximum along the Br—C axis near C as it splits into three separate points and now with negative values of $V_{s,max}$. The F_C σ-holes completely disappear at this smaller density.

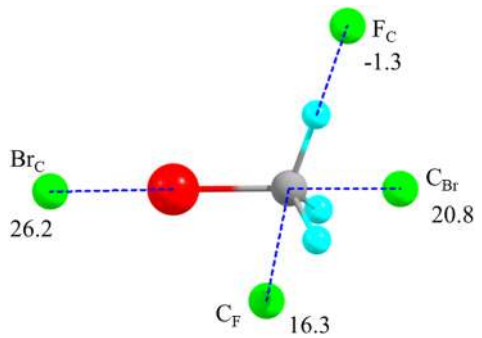

FIG. 4. Green balls representing positions of maxima of the MEP surrounding F_3CBr on a ρ = 0.001 a.u. isodensity surface. Numbers indicate the value of MEP at that point in kcal/mol.

One could also go in the opposite direction, closer to the atoms by using a larger value of ρ. In the particular case of ρ = 0.005 a.u., these points are brought in closer toward the nuclei of the molecule. For example, the Br_C σ-hole maximum lies only 1.63 Å from the Br atom. Lying closer to the nuclei and subject to less electron shielding, all of the $V_{s,max}$ become more positive. The Br_C maximum remains the largest but only by a thin margin, 55.5 kcal/mol vs 55.1 kcal/mol, over the C_{Br} maximum that would result in a tetrel bond if utilized. The other maxima around the C atom, along the F—C bond extensions, are still present and only slightly less positive at 50.0 kcal/mol. The F_C σ-holes finally turn positive for ρ = 0.005 a.u., at +4.4 kcal/mol.

There are more extreme cases of high sensitivity to the choice of isodensity ρ. In one example,[117] the change from 0.001 a.u. to 0.002 a.u. led to opposite sign of certain charges. In a more recent case,[105] the adjustment of the density surface moved not only the distance but also the angular orientation of MEP extrema.

So all in all, the picture presented by location and quantification of the minima on an isodensity surface can be a subjective one, which undergoes certain changes as one moves further away from the molecule by reducing the value of ρ. CF_3Br is not an outlier in this regard as there are other examples where the particular choice of ρ can cause reorientation of the positions of the MEP extrema.[105,118] It would therefore be judicious to bear these ideas in mind when assessing the locations and strengths of σ-holes for a given system.

Hence, the question that comes immediately to mind is which isodensity surface would be most appropriate. The answer depends on what it is the researcher wishes to know. If the issue at hand is what would be the proper, lowest energy trajectory for an incoming nucleophile, a proper answer would then be to use a different surface for each different distance as the nucleophile approaches. In other words, a small ρ would best characterize what the base sees from a longer distance, but this density should be progressively increased as the base comes ever closer. While the values of each maximum would increase during this operation, it is hoped that their relative values would remain unchanged. The CF_3Br molecule is a case in point. Regardless of the value of ρ chosen, from 0.000 01 all the way up to 0.005 a.u., and for distances of the point of reference to the Br atom dropping from 3.12 Å to 1.63 Å, it was the Br_C σ-hole that was the most intense as compared to the other types. One would thus be able to predict that the CBr···N halogen bond is likely to be preferred over any tetrel or F-halogen bond. The question would obviously be more nettlesome were these maxima to shift their relative magnitudes for different density surfaces.

Of course, this scheme offers no more than a prediction. As the molecules approach to within the bonding distance, the value of $V_{s,max}$ at a single point becomes less and less relevant as it is the entire electronic density distribution that determines the full electrostatic contribution. Moreover, the electrostatic term is only one of several attractive contributions that enter into the full interaction energy. The two molecules perturb one another's electron clouds as they approach, making the electrostatic interaction of the unperturbed clouds less relevant. It is for that reason that induction and dispersion must be accurately assessed as important elements of the interaction. In the context of the $CF_3Br···NH_3$ complex, in its optimized complex, with R(Br···N) = 2.900 Å, the electrostatic component of 10.0 kcal/mol is smaller than the 16.4 kcal/mol arising from induction, with an additional 3.7 kcal/mol attributed to dispersion. These various attractive forces are all opposed by exchange repulsion, which amounts to 27.0 kcal/mol.

B. Electron density shifts

The electrostatic interaction term allows no adjustment of electron clouds as the two molecules approach one another. However, clearly, such adjustments do take place. A pictorial version of this adjustment is illustrated in Fig. 5 for four different intermolecular distances within the $F_3CBr···NH_3$ halogen-bonded complex. In each case, the purple regions indicate areas where the electron density is increased as a result of the approach of the two units toward one another, while density losses are represented by yellow contours. Specifically, each diagram was generated by taking the density of the entire complex as shown and then subtracting out the density of each monomer in the absence of the other, i.e., its unperturbed density.

Even at the very long intermolecular distance of 10 Å, one can see some polarization beginning. Of course, in order to visualize these small changes, one has to consider miniscule density changes of only 0.000 02 a.u., but the changes are visible all the same. There is a yellow area of density loss on both sides of the Br atom but a gain along the C—Br axis closer to the C atom. There are also polarizations of the three F substituent atoms, a loss near the nucleus and gains on either sides of the C—F bond axis. One can also see the beginnings of a density loss from the lone pair region of the base N atom.

As the two molecules approach more closely to one another, the patterns remain in place, even if their magnitude grows. At the 6.0 Å distance, the density difference contour required to see the changes in Fig. 5 is reduced down to 0.0001, and it is becoming clear that there is some density loss also on the far side of the N atom, directed away from the Br atom, but the scheme is otherwise unaltered. An even smaller density difference level of 0.0005 a.u. is needed for R = 4.0 Å, and when the two molecules have reached their equilibrium intermolecular distance of 2.9 Å, Δρ need only be 0.001 a.u.

While the patterns in the figure provide a detailed three-dimensional picture of charge motion, they lack a certain degree of quantitative measure. For this purpose, one can turn to schemes whereby the electron density is assigned to particular atomic centers. However, how exactly should the total density be assigned to individual nuclei? There are quite a number of ways of doing so in the literature, but probably the most common are Mulliken and NBO prescriptions.

These atomic charges are displayed in Table II for purposes of comparison. The first two columns refer to the fully optimized and separate F_3CBr and NH_3 monomers and indicate very substantial differences between the two formulations. The C atom is assigned a much more positive charge in the NBO than in the Mulliken scheme, and the F atom is assigned a more negative charge. The N atom of

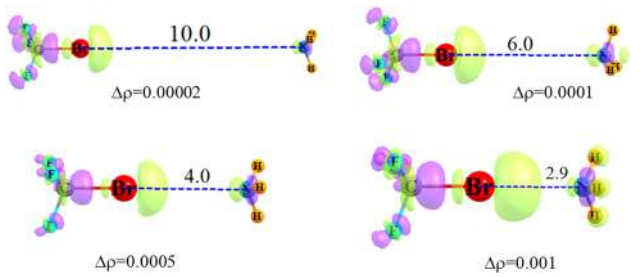

FIG. 5. Electron density shifts resulting from F_3CBr and NH_3 monomers approaching one another, with R(Br···N) shown in Å. Purple and yellow regions indicate gains and losses of density, respectively.

TABLE II. Mulliken and NBO atomic charges of optimized separate monomers, $F_3CBr···NH_3$ complex, and their difference, all in e.

	Monomers		Complex		Complex—monomer	
	Mulliken	NBO	Mulliken	NBO	Mulliken	NBO
Br	0.015	0.059	0.092	0.093	0.077	0.034
C	0.683	0.985	0.642	0.960	−0.041	−0.025
F	−0.233	−0.348	−0.248	−0.359	−0.015	−0.011
Sum	−0.000	0.000	−0.010	−0.025		
N	−0.917	−1.190	−0.951	−1.201	−0.034	−0.011
H	0.306	0.397	0.320	0.409	0.015	0.012
Sum	0.000	0.000	0.010	0.025		

NH_3 is also quite a bit more negative for NBO, and the H atom is more positive. (The reader should be aware that there are also cases where two different means of assessing atomic charges provide opposite signs for certain atoms.)

The next two columns refer to the full $F_3CBr\cdots NH_3$ complex. The differences in each atomic charge caused by the complexation are contained in the last two columns, and it is these changes that are most important. In fact, the two very different prescriptions offer fairly similar pictures of the changes in atomic charge. The C atom of F_3CBr becomes more positive, while the F and Br atoms both become more negative. Likewise, for the NH_3 unit, N and H atoms become, respectively, more negative and positive, regardless of the scheme. So, the atomic charges paint a picture wherein electron density is withdrawn from C and moved over to its Br and F substituents; density moves from H to N in NH_3, albeit in smaller quantities. However, the quantitative aspects are a bit different. In this particular case, the NBO charge changes are a bit less than those from the Mulliken formalism. However, this will not always be the case. There are some that argue that NBO generally overestimates charge transfer, as, for example, in halogen bonding.[119]

These atomic charge changes are at least partially consistent with the three-dimensional diagrams in Fig. 5. The greater positive charge on the Br atom is reflected by the yellow density losses surrounding this center. The lowered positive charge on the C atom is manifested by the large purple density gain region to its immediate right, just as the more negative F charges are visualized by the purple regions around these nuclei. The charge changes in NH_3 are a bit smaller in Table II but nonetheless are visible in the plot. The purple density gains around the N reflect the greater negative charge on the N atom, just as the more positive charge on the H atom is visible as the surrounding yellow contours.

There is some debate in the literature concerning the distinction between polarization and charge transfer. What is meant by this question is that polarization refers to internal rearrangements of electron density within the confines of a single molecule. Charge transfer, on the other hand, corresponds to density that transfers across from one molecule to the other, in either direction. Inspection of Fig. 5 illustrates the problem with trying to make such a distinction. Where exactly should the border between the two molecules be drawn? One option might be a plane, perpendicular to the Br···N axis. But even so, where should this plane be located, at the Br···N midpoint? At the point where their vdW radii intersect? Since the distribution of density around any atom within a molecule is nonspherical, can a single radius capture the density accurately? Or perhaps, the confines of each molecule could be taken as a surface comprising the vdW radius of each atom. But then, what about the space not covered by either molecule in such a scheme? In any event, this issue is mentioned here in order to warn the reader against any claims in the literature that charge transfer and polarization effects have been calculated separately. Yes, that can be done, but only under certain arbitrary definitions, which must be carefully elucidated and described. It is far more common to make no attempt at such a distinction and to simply lump the two together under various umbrellas such as induction, orbital interactions, or (perhaps misleadingly) polarization.

On the other hand, even if an evaluation of the energetics of charge transfer is a tall order, one can measure this quantity in terms of the total charge transferred between the two molecules. This task is usually accomplished by summing up the charges assigned to each atom within one subunit or the other. Of course, this sort of calculation contains within itself the same arbitrariness as in the calculation of the atomic charges themselves, but the hope is that although different schemes might provide different atomic charges, their *changes* might be less subjective. Indeed, the data in Table II did reflect that hope, in that both Mulliken and NBO schemes provided similar changes in atomic charges upon complexation.

The rows in Table II labeled as sum report the total of all atoms within a given subunit, whether F_3CBr or NH_3. These sums are of course zero for the isolated neutral monomers. However, that is no longer the case in the complex since some amount of charge can be transferred between them. Taking the Mulliken data first, the total charge on the F_3CBr subunit is −0.010 (and that of NH_3 is of course +0.010), which indicates that 0.010 electrons have transferred from the latter to the former, which is consistent with the idea of charge transferring from the N lone pair to σ^*(CBr) antibonding orbital. The direction of transfer is the same in the NBO scheme, but the amount is somewhat larger at 0.025*e*. So, the two schemes differ not in the direction of charge but in the amount. It is difficult to visualize this transfer in the pictorial version of Fig. 5. Both molecules show both purple and yellow regions, and it is not at all obvious that which will predominate. So, researchers typically depend on some atomic orbital assignment scheme or other to (i) define the direction of transfer and (ii) provide a quantitative estimate of this amount.

The displacements of electron density that arise due to the interaction have an energetic consequence. Most energy decomposition schemes calculate this component, so comparison may be made with electrostatic or other energetic contributions. This induction term can be seen as the green curve in Fig. 1 to be very short range. It is only below about 5 Å that the induction term becomes appreciable, although still far less negative than the full electrostatic term. However, the induction term rises quickly in magnitude as R is further reduced. At the equilibrium separation of R = 2.9 Å, the induction energy is larger than the electrostatic term, 13.9 kcal/mol vs 8.5 kcal/mol. So, induction can be extremely important but dies off quickly with the intermolecular distance.

The preceding has discussed overall density shifts that encompass all orbitals of each molecule. However, most of these noncovalent bonds have one particular charge transfer that plays a dominant role. In particular, a certain amount of density is transferred out of the lone pair orbital of the electron donor atom of the nucleophile, as in $F_3CBr\cdots NH_3$. There are other sources for this transfer in the general case, for example, the π-systems of an aromatic system such as benzene[120,121] or simple π-bonds.[122–125] Another, although rarer source, is the σ bond orbital, as in, for example, H_2,[107,126] B_2H_4,[127,128] or B_4H_4 or B_4Me_4.[129] The dominant destination of this density is the σ^* antibonding orbital of the Lewis acid, which here would be the σ^*(CBr) orbital. The Natural Bond Orbital (NBO) scheme[130,131] is able to quantify this amount of density and, more importantly, its energetic consequence in the form of a second-order perturbation energy E(2). This energetic quantity is of even shorter range than the full induction. In our exemplary case of $F_3CBr\cdots NH_3$, it only reaches a quantifiable amount for R = 4 Å, at which point it is only 0.23 kcal/mol, only half of the total induction energy. In the optimized geometry, where R = 2.9 Å, the NBO value of E(2) is 6.5 kcal/mol, only 40% of E_{ind} = 16.4 kcal/mol.

C. Dispersion and exchange

The purely electrostatic and induction forces are not the only ones that need to be considered. London dispersion forces come into play as well. Dispersion is fairly isotropic (although not completely so[132]) and so is not heavily involved in the molecular orientation. However, it nevertheless can make a substantial contribution to the total attraction, particularly in the case of larger, more polarizable atoms that occur lower in the periodic table. Another example arises when the source of the charge to be transferred is associated with the highly polarizable π-clouds of aromatic systems.

With all of these attractive forces, why does the bimolecular system not simply collapse to a single molecule? The force that tends to hold them apart is due to electron exchange, which may be thought of as the simple steric repulsions between electron pairs on the two molecules. Exchange is of very short range, with many molecular mechanics force fields employing a simplified R^{-12} approximation. Because the individual orbital contributions to the electron density are anisotropic, exchange can exert a profound effect on the angular dependence of the noncovalent bond energy. It has been shown, for instance, to be a controlling factor in the strong tendency toward linearity in H-bonds and the other noncovalent bonds discussed here.[133–137]

V. NON-ENERGETIC MEASURES OF BOND STRENGTH

A. Structural

In the field of crystallography, individual intermolecular energies are inaccessible, and the principal data refer instead to structural details. One is thus forced to base judgment as to the presence of a noncovalent bond on geometrical aspects. It is logical then that the most common criterion used to make this decision is whether the two atoms in question are located closer together than their vdW radii. Furthermore, the more these two atoms have penetrated one another's "personal space," the stronger the interaction is thought to be. This concept makes a good deal of logical sense but is of course subject to some uncertainty. For example, two atoms may be forced close together, even without an attractive interaction, by crystal packing forces or intramolecular forces that are far removed from their immediate vicinity. In cases such as this, it would be misleading to refer to a noncovalent bond, even upon close contact. Conversely, even if two atoms are spaced further apart than their vdW radii sum, that is, insufficient grounds, so assert that there is no attractive interaction between them.

B. Electron density topology

In addition to the energy required to pull a noncovalent bond apart into its two constituent species, there are also other ways that have been devised to measure their strength. A principal method in this regard is Bader's Quantum Theory of Atoms in Molecules (QTAIM, or sometimes just AIM) that places its emphasis on the topology of the electron density.[138] Consideration of its gradient and Laplacian allows the identification of bond paths between atoms. One can think of this path in terms of a mountain ridge between two towns, each perched on the top of a hill. These towns represent the atoms, with high electron density. In walking along the ridge, one is surrounded by a falloff on either side. Upon leaving the first town along the path, one begins to descend, until the approximate midpoint, at which time an ascent begins. The low point, a stationary point, where the Laplacian contains two negative and one positive eigenvalue, is called the bond critical point (BCP), and its properties are commonly used to assess the strength of the bond between the two atoms. The definition of such a BCP is that the density Laplacian at that point ought to have two negative and one positive eigenvalue, referred to as (3,−1) in AIM parlance. Also of interest is the Laplacian of the density at this critical point. A positive Laplacian signals charge depletion, typical of noncovalent bonds, whereas charge accumulation is suggestive of a possible covalent bond.

Taking the $F_3CBr\cdots NH_3$ system as our example again, the eigenvalues of the density Laplacian are calculated to be −0.014, −0.014, and +0.008, at the bond critical point connecting the Br and N atoms, conforming to the requirement. The density of the bond critical point, ρ_{BCP}, is equal to 0.0186 a.u. This quantity is typical of a noncovalent bond, for which the unofficial maximum is on the order of 0.100 a.u.; larger values are thought to signal the transition to a covalent bond. For example, ρ_{BCP} = 0.169 a.u. for the covalent C—Br bond in this complex and 0.283 a.u. and 0.388 a.u. for the C—F and N—H covalent bonds, respectively. Other properties of the BCP that are sometimes reported are the Laplacian at that point, which is equal to +0.0059 for $F_3CBr\cdots NH_3$. As mentioned above, it is usually thought that a positive value such as this is characteristic of a noncovalent bond, whereas it will turn negative if the bond is covalent. V and G refer to the AIM potential and kinetic energy densities, respectively, which here are −0.0119 a.u. and +0.0136 a.u. A value significantly below unity for −G/V, here equal to 1.14, is sometimes taken as a sign of a covalent bond.[139] Another quantity frequently alluded to is the total energy density H, equal to the sum of G + V. A positive H, here equal to +0.0017 a.u., is indicative of noncovalent character.

The presence of a bond path between two atoms, even if ρ_{BCP} is quite small, is commonly used as a litmus test as to whether or not such a bond is present. Applying this idea to the $F_3CBr\cdots NH_3$ complex, ρ_{BCP} drops from 0.0186 a.u. for R = 2.9 Å in the optimized geometry down to 0.0024 upon stretching the two molecules apart to 4.0 Å. It continues to diminish upon further stretching, until the bond path disappears entirely for R > 6 Å. So, in this case, the AIM criteria would suggest that the halogen bond switches off at 6 Å, at which point the binding energy is still 1.0 kcal/mol. To place this threshold in perspective, as mentioned earlier, the NBO finding of a measurable transfer of charge from the N lone pair to the σ^*(CBr) antibonding orbital only occurs for R < 4 Å, at which point the bond energy is as high as 3.3 kcal/mol. So, one might conclude that NBO has a stricter threshold than AIM, which occurs at a longer intermolecular distance, with a bond energy that is still quite significant.

There are many noncovalent bonds of interest in which the two groups are located on the same molecule. An obvious example would be the NH···O H-bonds within a single strand of α-helix of a protein. The definition of interaction energy fails in such intramolecular cases as one cannot pull this bond apart without also breaking covalent bonds elsewhere and thereby completely disrupting the system. However, one of the principal strengths of the AIM analysis of noncovalent bonds is its ability to consider intramolecular bonds

on precisely the same footing as intermolecular correlates. AIM bases its analysis on the total electron density, whether a single entity or a pair of molecules.

Another strong point of AIM is that it is based upon the electron density. While this property is typically evaluated by quantum chemical means, it is also subject to determination via experimental x-ray structure methods[140,141] and so can connect theoretical with experimental data.

However, despite its high diagnostic value, AIM is also subject to certain weaknesses of which a user must be aware.[142,143] There are numerous cases in the literature where an AIM bond path was identified within a given system but where a noncovalent bond was clearly not present.[144–150] The converse is also true where AIM fails to locate a bond path between two noncovalently bonded atoms.[151,152] Another issue relates to noncovalent bonding, not to a lone pair electron donor but rather to a π-cloud, e.g., a phenyl ring.[153] AIM has a marked proclivity toward atom–atom interactions, even when such a picture might be misleading. So, when a halogen atom in a RX bond is brought toward a phenyl ring, it is typical for AIM to designate bond paths leading to more than one of the C atoms, rather than present a bonding picture that involves the entire aromatic π-system.

C. Spectroscopic

In addition to adjustments of the electron density to the mutual effects of the two monomers upon one another, there are other perturbations as well. For one thing, the internal geometry of each monomer will change as the other subunit approaches, as will the vibrational and NMR spectra.[154–160] An illustration of these changes as the F_3CBr and NH_3 molecules approach one another to engage in a halogen bond is provided by the data in Table III. The values listed refer to the change in each quantity relative to the isolated and fully optimized monomer.

The interaction causes a contraction in the internal C—Br bond. This contraction starts off quite small at only 1 mÅ for R = 10 Å but grows to as much as 8 mÅ for R = 3.5 Å. As the intermolecular distance shrinks the last little bit to 2.9 Å, the pattern reverses as the C—Br bond contraction reduces to only 3 mÅ. Except for the very small initial red shift at R = 10 Å, the C—Br stretching frequency undergoes a progressively larger blue shift that culminates in an increase of 21 cm^{-1} in the equilibrium geometry. A shift in this direction is not unusual in XBs,[155,161–164] just as it is known to occur in certain HBs.[95–99,165–168]

TABLE III. Changes in the C—Br bond length and stretching frequency, and NMR chemical shielding caused by complexation in $F_3CBr\cdots NH_3$.

			Δσ (ppm)		
R(N···Br) (Å)	Δr (Å)	Δν (cm^{-1})	Br	N	C
2.9	−0.0030	21.2	78.53	−8.01	0.25
3.5	−0.0081	12.7	29.02	−0.34	−1.95
4	−0.0079	11.2	−6.15	0.43	−0.54
5	−0.0065	8.3	−12.74	0.31	−0.39
6	−0.0048	4.5	−3.19	1.30	−0.24
7	−0.0024	1.1	−3.06	1.03	−0.12
8	−0.0032	2.2	1.22	−0.76	0.06
10	−0.0010	−1.4	−2.43	0.13	0.04

TABLE IV. Maximum value of the electrostatic potential (kcal/mol) on the isodensity surface corresponding to ρ = 0.001 a.u.

	$V_{s,max}$ (C_H)		$V_{s,max}$ (C_F)	
	TH_4	TF_3H	TH_3F	TF_4
T = C	. . .	10.14	21.31	24.95
T = Si	19.39	34.80	41.13	49.98
T = Ge	17.80	34.22	45.06	58.76
T = Sn	24.25	45.40	53.67	74.52

The gradual formation of the halogen bond also causes changes in the NMR chemical shielding of the various atoms. These changes are exhibited in the last three columns of Table III for the directly interacting Br and N atoms, as well as the C atom to which the Br atom is attached. A graphical view of these changes in Fig. 6 emphasizes that these changes are neither smooth nor uniform as R changes. The Br shielding is increased by nearly 80 ppm in the equilibrium geometry of R = 2.9 Å. It then decreases rapidly, turning negative, until reaching a maximum deshielding of −13 ppm at R = 5 Å. As the intermolecular distance increases further, the deshielding is reduced, with some oscillations along the way.

The changes in the C and N shielding are much smaller in magnitude, mostly less than 1 ppm, but nonetheless display certain oscillations as well. The N atom, for example, suffers an 8 ppm deshielding in the equilibrium geometry, which reverses into a small shielding for longer R. Except for a 2 ppm deshielding at R = 3.5 Å, the C nucleus undergoes a much smaller deshielding for all other intermolecular distances. An exception is the equilibrium geometry where the C atom is slightly shielded relative to the monomer.

These irregular fluctuations in the NMR shielding cannot be easily attributed to similar fluctuations in the electron densities surrounding these atoms. Figure 5 has shown that the changes in

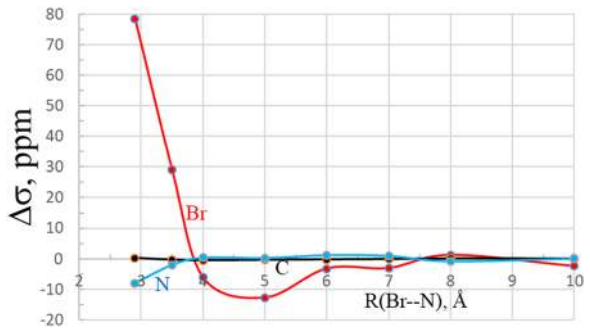

FIG. 6. Changes in chemical shielding within $F_3CBr\cdots NH_3$ as two molecules approach one another.

density are quite regular as R is changed. On an atomic level, the changes in the natural atomic charges are also a smoothly changing function of R. The atomic charge of the Br rises steadily by 0.032*e* as the two molecules approach to their equilibrium geometry, while both N and C become more negative by 0.011*e* and 0.025*e*, respectively, again monotonic functions of R. These changes in the overall atomic charge do not comport with a simple interpretation of Δσ. For example, the loss of total density on the Br atom might lead one to expect a deshielding, but there is in fact a large increase of shielding.

This is one area where the XB differs from the simpler HB. In the latter case, the bridging proton suffers a loss of density and a rise in positive charge as the HB is formed, similar to that of the bridging Br atom in the XB. However, this charge loss culminates in H deshielding but Br shielding. Another clear distinction is associated with the C—Br bond length and stretching frequency shift in Table III. Unlike the CH stretching and red shift characteristic of a HB, the C—Br bond contracts and shifts to the blue. On the other hand, it is important to note that HBs do not always shift to the red. There is a subclass of such bonds where the opposite effect of a bond contraction and blue shift occurs instead.[93–100]

D. Geometric deformations of monomers

As alluded to above, the coming together of a pair of monomers to engage in a noncovalent bond causes certain changes in their electronic and spectral characteristics. Internal structures also change, i.e., nuclear rearrangements, for example, the contraction of the C—Br bond in $F_3CBr\cdots NH_3$. In this particular complex, this bond contracts by 0.003 Å, a not unusual occurrence in XBs.[169] There are other changes as well. For example, r(CF) elongates by 0.006 Å and the θ(BrCF) angles undergo a small increase of 0.7°. Within the NH_3 subunit, r(NH) stretches slightly by 0.001 Å and the θ(HNH) angle diminishes by a scant 0.2°. These geometric adjustments induce very little change in energy. The deformation energy required by F_3CBr to adopt the structure it acquires in the complex is only 0.14 kcal/mol and that of NH_3 is even less at 0.003 kcal/mol. So, together, this total E_{def} hardly affects the total interaction energy, lowering it from 7.18 to a binding energy E_b of 7.03 kcal/mol.

The preceding represents the situation in the majority of noncovalent bonding systems, where the geometries of the monomers change only a little upon engaging in the complex, with a consequent small deformation energy, which, in turn, results in a fairly close equivalence between interaction and binding energy. However, this is by no means the situation in all such noncovalent bonds. Tetrel bonds provide a notorious counterexample. Tetrel atoms (T = C, Si, etc.) generally find themselves in a tetravalent bonding situation with four R substituents TR_4, within a tetrahedral structure. Each of the four T σ-holes, opposite one of the R groups, lies on a face of the tetrahedron, with the three surrounding R groups only some 70° away. These cramped quarters make it difficult for a base to approach the σ-hole, unless it is able to pry apart the nearby R groups.[102,170,171] In so doing, the tetrahedral structure is distorted into something more akin to a trigonal pyramid, which, in turn, engenders a substantial deformation energy.

An example of this situation is provided by a study[172] of the complexation of NH_3 with a series of tetrel-containing small molecules beginning with TH_4 and then progressing with higher degrees of fluorosubstitution. Each replacement of H by electron-withdrawing F ought to strengthen the σ-hole. The first two columns of Table IV refer to the σ-hole opposite the H atom of TH_4 and TF_3H, while the C_F hole is represented in the last two columns. In either case, the replacement of the three H atoms by F atoms very substantially increases $V_{s,max}$. The other trend is the intensification of the σ-hole as the T atom grows larger, with the exception of the near equivalence for Si and Ge for the C_H hole. Note also the absence of any σ-hole at all in the unsubstituted CH_4 molecule.

TABLE V. Binding energy E_b of the indicated σ-hole of Lewis acid with NH_3, kcal/mol.

	C_H		C_F	
	TH_4	TF_3H	TH_3F	TF_4
T = C	...	...	−1.84	−0.82
T = Si	−1.66	−4.75	−5.49	−10.59
T = Ge	−1.48	−8.68	−5.84	−16.77
T = Sn	−2.44	−18.20	−8.51	−25.53

The energetics of the binding process are outlined in Table V that generally follow the trends of the σ-hole. Beginning with T = C, neither CH_4 nor CF_3H, with their nonexistent or shallow CH σ-hole is capable of engaging in a TB, whereas the deeper CF σ-holes opposite the C—F bond can sustain such a bond. The progressive enlargement of T to Si, Ge, and then Sn strengthens these interactions, most notably for the fully fluorosubstituted TF_4, for which $F_4Sn\cdots NH_3$ reaches a peak E_b of over 25 kcal/mol.

However, these bonds come at a cost. As NH_3 moves in closer to the Lewis acid, the three adjacent substituents, whether H or F, must be moved aside. The originally tetrahedral TR_4 species distorts into a trigonal pyramid, a process that can be measured by the $\theta(R_1TR_2)$ angle where R_1 refers to the substituent opposite NH_3 and R_2 refers to one of the others. This angle would be 109.5° in the fully tetrahedral system but only 90° in a fully formed pyramid, a change of −19.5°.

The actual change in this angle occasioned by the formation of the complex of each Lewis acid with NH_3 is reported in the left half of Table VI. The reduction in this angle is fairly small when it is three H atoms that must be displaced, 5° or less, but it is quite substantial for prying apart three F atoms, on the order of 13°. The

TABLE VI. Angular distortion imposed on the Lewis acid molecule by formation of a complex with NH_3 and the resulting deformation energy.

	$\Delta\theta(R_1TR_2)$ (deg)				E_{def} (kcal/mol)			
	C_H		C_F		C_H		C_F	
	TH_4	TF_3H	TH_3F	TF_4	TH_4	TF_3H	TH_3F	TF_4
T = C	...	...	0.1	−0.6	...	...	0.02	0.06
T = Si	−1.4	−12.6	−4.9	−12.7	0.14	21.38	1.93	20.78
T = Ge	−1.2	−12.9	−4.6	−12.5	0.11	18.99	1.51	16.61
T = Sn	−2.5	−12.0	−5.3	−11.0	0.37	12.50	1.77	9.62

TABLE VII. Interaction energy E_{int} of the indicated Lewis acid with NH_3, kcal/mol.

	C_H		C_F	
	TH_4	TF_3H	TH_3F	TF_4
T = C	...	...	−1.86	−0.88
T = Si	−1.80	−26.13	−7.42	−31.37
T = Ge	−1.59	−27.67	−7.35	−33.38
T = Sn	−2.81	−30.70	−10.28	−35.15

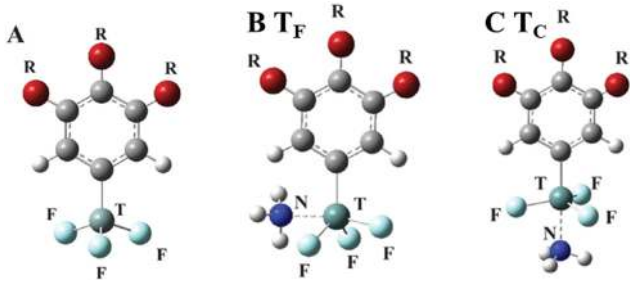

FIG. 7. (a) Geometry of the F_3TPhR_3 monomer and geometries of complexes with NH_3 in the (b) equatorial and (c) axial positions.

right-hand side of Table VI details how much this angular change (in addition to various bond length changes not explicitly listed here) causes the energy of the monomer to rise. For the small geometrical distortions of TH_4, E_{def} amounts to less than 0.4 kcal/mol and rises slightly toward 2 kcal/mol if the three H atoms reside on TH_3F. However, these deformation energies are very substantial indeed for parting three F atoms by the required 13°. For T = Si and Ge, there is 17 kcal/mol–21 kcal/mol cost and slightly less for the largest Sn atom. Indeed, there is a general rule exemplified here that deformation energies tend to diminish as the central T atom becomes larger. The obvious exception is T = C because the TB is so weak.

The interaction energy is defined with the monomers already in their pre-deformed geometries and so do not have this energetic cost. E_{int} is consequently larger (more negative) than the binding energies by this amount (plus a very small increment that would also include deformation of the base, which is very small here). It is readily apparent from Table VII that these interaction energies can be quite sizable, as in the 35 kcal/mol value for the most strongly bound $F_4Sn\cdots NH_3$.

It is not uncommon that E_b and E_{int} do not obey the same precise trends. These systems are a case in point. Both energetic measures are consistent with a growing bond strength for larger T. Both also agree that there is a stronger interaction when the three R_2 substituents are changed from H to F. Where they differ is in degree. Whereas the latter trisubstitution enhances E_b by some 3 kcal/mol–10 kcal/mol, and a bit more for Sn, the effects of the three F atoms are more dramatic in terms of E_{int}, especially for the smaller T atoms, where it can amount to more than 20 kcal/mol.

Given the numerical differences between E_b and E_{int} when there is a large deformation, it becomes relevant to ask which is a better gauge of the strength of the interaction. The answer depends on what specifically one wants to know. E_{int} may perhaps best be thought of as the raw and unadulterated strength of the interaction itself. E_b, on the other hand, also takes into account other factors that cannot be ignored in the actual reaction itself, the geometrical deformations that each subunit must go through in order to achieve the goal of a fully formed complex.

VI. COMPETING BINDING SITES

A. Chemically different sites

The deformation energy can play an outsized role in the competition as to where exactly a noncovalent bond will be formed. As an example, consider the situation where a T atom is covalently attached to three F atoms and an aromatic ring, as depicted in Fig. 7(a). The particular choice of the three R substituents on the phenyl ring can adjust its electron-withdrawing capacity and the magnitude of the σ-hole it induces on the central tetrel T atom directly opposite this ring.[173] However, there will also be σ-holes lying opposite each of the three F atoms, so an incoming base would have a choice as to which of these holes to choose in the formation of a tetrel bond. The intensities of the various σ-holes contained in Table VIII follow the expected trends that an electron-withdrawing F substituent on the aromatic ring will intensify $V_{s,max}$, and there is also a general trend for stronger σ-hole with a larger T atom. However, the most important aspect of the data with regard to the competition is that it is the C_F σ-hole that is favored over C_C in all cases and by a substantial margin. So, one would anticipate that a base would prefer the former position.

TABLE VIII. Molecular electrostatic potential maxima (in kcal/mol) on the 0.001 a.u. isodensity surface of the electron density ($V_{s,max}$) of $TF_3C_6H_2R_3$ monomers.

	C_F	C_C
$CF_3C_6H_5$	8.6	1.4
$CF_3C_6H_2F_3$	17.8	9.9
$CF_3C_6H_2(CH_3)_3$	5.0	−2.1
$SiF_3C_6H_5$	31.8	25.4
$SiF_3C_6H_2F_3$	42.0	35.1
$SiF_3C_6H_2(CH_3)_3$	27.4	21.0
$GeF_3C_6H_5$	38.3	23.4
$GeF_3C_6H_2F_3$	46.3	32.0
$GeF_3C_6H_2(CH_3)_3$	33.6	19.0
$SnF_3C_6H_5$	54.3	33.2
$SnF_3C_6H_2F_3$	64.9	44.3
$SnF_3C_6H_2(CH_3)_3$	46.6	28.3
$PbF_3C_6H_5$	53.7	18.5
$PbF_3C_6H_2F_3$	64.5	29.0
$PbF_3C_6H_2(CH_3)_3$	49.1	13.3

TABLE IX. Binding, interaction, and deformation energies (kcal/mol) of $TF_3C_6H_2R_3$ complexes with NH_3.

	E_b		E_{int}		E_{def}	
	T_F	T_C	T_F	T_C	T_F	T_C
$SiF_3C_6H_5$	−4.45	−2.14	−18.59	−24.94	14.14	22.81
$SiF_3C_6H_2F_3$	−5.64	−5.29	−20.93	−28.50	15.29	23.20
$SiF_3C_6H_2(CH_3)_3$	−3.94	−0.90	−17.89	−23.71	13.95	22.81
$GeF_3C_6H_5$	−8.22	−6.33	−20.42	−26.94	12.20	20.61
$GeF_3C_6H_2F_3$	−9.69	−9.42	−23.01	−29.88	13.32	20.47
$GeF_3C_6H_2(CH_3)_3$	−7.75	−5.11	−19.81	−25.91	12.06	20.79
$SnF_3C_6H_5$	−17.02	−17.77	−24.06	−32.55	7.04	14.78
$SnF_3C_6H_2F_3$	−18.87	−20.40	−26.24	−33.84	7.28	13.44
$SnF_3C_6H_2(CH_3)_3$	−16.43	−16.46	−23.28	−30.43	6.84	13.97
$PbF_3C_6H_5$	−15.11	−17.66	−18.58	−30.79	3.47	13.12
$PbF_3C_6H_2F_3$	−16.71	−20.11	−19.97	−32.79	3.26	12.68
$PbF_3C_6H_2(CH_3)_3$	−14.29	−16.68	−17.20	−30.05	2.91	13.36

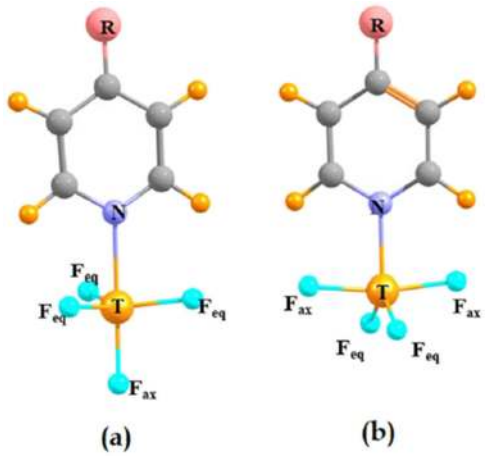

FIG. 8. (a) Axial and (b) equatorial sites for binding of a substituted pyridine to TF_4.

The calculated energetics exhibited in Table IX indicate a tight competition between the two sites. The overall formation exothermicities E_b favor T_F for the two smaller T atoms, but the preference switches over to T_C with the larger Sn and Pb atoms. In the context of the pure interaction energy E_{int}, on the other hand, there is a clear and universal preference for the T_C site. It is only the larger deformation energies for this site in the last two columns of Table IX that shift the equilibrium toward T_F for the smaller T atoms.

A major question then is why there seems to be a general preference for the T_C over the T_F site when it is the latter with the more intense σ-hole. The answer is related to the issue of steric crowding. The phenyl ring is of course more bulky than the F substituents. So, a T_F position for NH_3 is subject to more steric repulsion than a T_C position, as is clear in Figs. 7(b) and 7(c). As manifestation of this different level of congestion, the intermolecular R(T···N) distance tends to be shorter for the T_C complexes. This difference is roughly 0.08 Å for T = Si, rises to 0.10 Å for Ge and Sn, but then increases above 0.20 Å for Pb. So, the stronger T_C tetrel bonds for the heavier T atoms are associated in part with their shorter nature. The θ(C-T···N) angles are more linear than their θ(F-T···N) counterparts, shifting the energetic preference toward the T_C complexes. So, it is important to understand that the choice of optimal binding site is not solely dictated by considerations of the MEP.

B. Geometrically different sites

Another example[174] of a competition between two different binding sites arises in connection with the approach of a pyridine (Pyr) base to TF_4 as Lewis acid. According to the tenets of VSEPR that maximally spreads out electron pairs, the complexation will transition the central T atom from a tetrahedral tetravalent monomer to a pentavalent complex that will adopt a trigonal bipyramid shape. This geometry presents the system with two options. The Pyr base can adopt either an axial position, as illustrated in Fig. 8(a), or one of the three equatorial sites, as in Fig. 8(b). In order to register a guess as to which would be preferred, one can place the TF_4 molecule into an idealized trigonal bipyramidal structure, with a vacancy at either an axial or equatorial location. The values of $V_{s,max}$ for these two sites reported in Table X show a quite positive value, which will aid in the association with Pyr, with a slight edge toward the equatorial site.

This slight advantage in σ-hole intensity is dwarfed by the actual interaction energies in the next two columns of Table X, which are much larger for the equatorial location. This much higher proclivity toward the equatorial site resides in large part on steric repulsions. An equatorial site for the bulky pyridine suffers from lesser steric repulsions with its neighbors than when placed in an axial position. An equatorial Pyr can thus approach more closely to the central T atom, thereby allowing it to strengthen.

However, this greater intrinsic strength of the equatorial location comes with a strong caveat. As may be seen in the last two columns of Table X, it takes a great deal more deformation energy to distort the originally tetrahedral TF_4 into a trigonal bipyramid with an equatorial vacancy than with an empty axial site, in fact by a factor of two or more. Note also how quickly the deformation energy rises as the central T atom becomes smaller. This especially high deformation energy needed to carve out an equatorial vacancy for Pyr reverses the interaction energy order, making the axial conformer

TABLE X. Intensity of σ-holes in TF_4 monomers in trigonal bipyramid shape, and interaction and binding energies of complexes with pyridine, all in kcal/mol.

	$V_{s,max}$		E_{int}		E_b		E_{def}	
	ax	eq	ax	eq	ax	eq	ax	eq
SiF_4	120.6	126.5	−26.75	−50.09	−10.39	−0.98	20.70	53.87
GeF_4	116.4	120.1	−34.73	−52.02	−20.51	−14.60	20.07	44.09
SnF_4	124.3	131.4	−39.68	−50.66	−32.41	−29.14	13.38	27.69

preferred by between 3 kcal/mol and 10 kcal/mol. So, as in the previous case, the MEP alone is insufficient to accurately predict the relative energetics of two different sites to bind a base.

VII. MAXIMUM NUMBER OF BONDS

The number of σ-holes corresponds to the number of substituents covalently bonded to a central atom. So, whereas a univalent halogen atom has one such σ-hole, chalcogens, pnicogens, and tetrel atoms in their most common bonding situations would contain 2, 3, and 4 σ-holes, respectively. One can thus imagine that a central atom can in principle engage in a like number of noncovalent bonds simultaneously. On the other hand, the acquisition of each successive nucleophile will add a certain amount of electron density to the central atom, diluting the remaining σ-holes, which ought to weaken any additional bonds. So, it is legitimate to wonder if there is a maximum number of noncovalent bonds in which any central atom can engage.

A. Chalcogen bonding

The problem was considered from the vantage point of a hypervalent YF_4 molecule, where Y represents one of the S, Se, Te, or Po chalcogen atoms.[175] Given the five electron pairs that surround the central Y atom, including one lone pair, the molecule adopts a classic see-saw geometry, as illustrated in Fig. 9(a). As such, σ-holes can form along the extensions of the two equatorial F_e—Y bonds, which can each accommodate a base such as NH_3, as indicated in Fig. 9(b). This geometry is designated cis because the two bases lie *cis* to one another within the overall octahedral geometry of the complex. However, there is another alternative, pictured in Fig. 9(c) where the two NH_3 units lie *trans* to one another, in a distorted octahedron. One of the two bonds is designated as the π-hole because the base occupies a site above the plane of the YF_4 unit. The second NH_3 is loosely termed the σ-hole as it eschews the area above this plane and is roughly positioned to take advantage of the positive region opposite one of the F atoms.

The binding energetics are displayed in Table XI for purposes of comparison. With regard to the overall reaction energetics E_b, the *cis* complex is favored for the two lighter Y atoms but switches over to *trans* for Te and Po. The interaction energies in the next two columns tell a somewhat different story. Once the YF_4 unit has morphed from its original see-saw into the square planar shape needed for the *trans* geometry, the interaction energies are quite large, on the order of 50 kcal/mol. The difference, of course, resides in the very large energy needed to deform the see-saw YF_4 monomer into the square planar shape intrinsic to the *trans* complex. As indicated in the last columns of Table XI, these deformation energies vary from 18 kcal/mol for the largest Y=Po up to nearly 50 kcal/mol for Y=S. It is the smaller deformation energies of the larger Y atoms that allow for the overall preference of the *trans* structures.

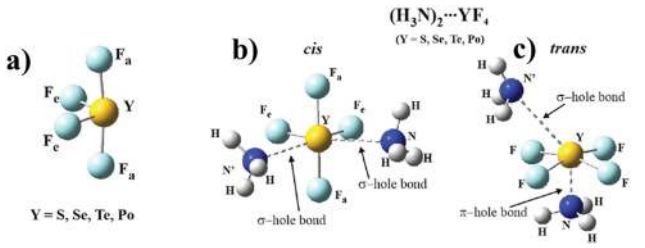

FIG. 9. YF_4 molecules as (a) the monomer and bound to a pair of NH_3 molecules in (b) *cis* and (c) *trans* orientations with respect to one another.

TABLE XI. Binding and interaction energies (kcal/mol) of complexes containing two NH_3 bases bound to a central YF_4 and the deformation energy required for monomers to adopt dimer geometries.

	E_b		E_{int}		E_{def}	
	cis	*trans*	*cis*	*trans*	*cis*	*trans*
SF_4	−11.21	−2.76	−13.10	−50.40	1.89	47.64
SeF_4	−17.16	−14.42	−20.15	−48.33	2.99	33.91
TeF_4	−22.62	−25.70	−28.82	−46.27	6.20	20.57
PoF_4	−32.37	−34.90	−37.17	−52.82	4.80	17.92

So, it is clear that these YF_4 molecules are all fully capable of engaging in two simultaneous YBs, formation of which is rather exothermic. However, these systems bring up the question of two alternative geometries, the preferred choice depending on the size of the central Y atom and the associated energy required to deform YF_4 into a square planar shape.

B. Pnicogen bonding

This same problem was engaged recently in the context of a central pnicogen atom Z. ZF_3 was taken[176] as the central trivalent molecule as the highly electron-withdrawing F atom should also maximize the intensity of the three σ-holes. Z atoms considered included the P, As, Sb, and Bi set, which also advanced a spectrum of σ-hole intensities. The choice of nucleophiles covered the full range of weak (NCH), medium (NH_3), and strong (CN^-). The results are summarized in Table XII, which display both the binding and interaction energies, their difference being the deformation energies required to mutate the geometry of each monomer from its fully optimized structure to that acquired within the context of the complex.

The results for the first section of data where n = 1 for a single nucleophile conform to the normal expectations for a pnicogen bond. The interaction and binding energies both climb as the Z atom becomes larger and more polarizable, and these energetics also are consistent with base strength NHC < NH_3 < CN^-. One important point is connected with the strong CN^- base, for which there is a very sizable difference between E_b and E_{int}. This difference signals a similarly large deformation energy that is attributed to a major rearrangement of the acid from the trigonal pyramid to a very nearly planar structure. These deformation energies ($E_b - E_{int}$) are particularly large for the smaller Z atoms.

When a second base is added, the energetics still follow these same principles. Note that the total interaction energies for n = 2 are not quite twice the values for n = 1 due to the negative cooperativity involved with a double electron-acceptor function of the

TABLE XII. Binding and interaction energies (kcal/mol) of complexes containing n bases bound to a common Lewis acid.

	NCH		NH_3		CN^-	
Lewis acid	E_b	E_{int}	E_b	E_{int}	E_b	E_{int}
n = 1						
PF_3	−2.74	−2.82	−4.45	−4.87	−22.68	−77.66
AsF_3	−4.09	−4.24	−7.32	−8.24	−30.93	−77.79
SbF_3	−5.88	−6.15	−11.70	−13.09	−38.67	−74.79
BiF_3	−7.48	−7.75	−13.20	−14.31	−39.24	−73.16
n = 2						
PF_3	−4.57	−4.70	−7.70	−8.66	...	...
AsF_3	−7.19	−7.51	−12.90	−14.88	...	...
SbF_3	−10.48	−11.06	−20.22	−23.28	+10.80	−4.29
BiF_3	−13.85	−12.86	−24.46	−27.45	−0.63	−12.92
n = 3						
PF_3	...	...	−10.14	−11.86	...	...
AsF_3	...	...	−17.39	−20.64	...	...
SbF_3	...	...	−27.15	−34.68	...	...
BiF_3	...	...	−34.43	−40.24	...	...

central molecule. Most interesting is the fact that neither PF_3 nor AsF_3 are able to engage in a stable complex with two CN^- anions. This is sensible in light of the fact that binding of the second anion would have to counteract a destabilizing anion–anion interaction with $F_3Z\cdots CN^-$. The two larger Z atoms, on the other hand, are able to manage to bind a second anion. This ability can be traced to the stronger Lewis acidity of the larger Z atoms. But even so, the interaction energies are far less negative than the values associated with binding of the first anion. Because of the high deformation energies that are characteristic of the CN^- interactions, E_b is either close to zero or even positive for $F_3Sb\cdots(CN^-)_2$.

Particularly interesting is the attempt to form a third ZB. The very high electrostatic repulsion between a $F_3Z\cdots(CN^-)_2$ dianion and CN^- is simply too strong to overcome. The weaker NCH can squeeze in a third ligand, but its very low nucleophilicity causes the third molecule to rotate around and engage in an NCH···F HB instead. It is only the NH_3 base, whose "Goldilocks" medium strength enables it to form a third ZB and thereby fully occupy all three ZF_3 σ-holes. The energetics listed in the lowest section of Table XII continue to conform to the expected dependency on the size of the Z atom.

So, the filling of all three σ-holes surrounding a pnicogen atom is possible but only under certain conditions. The base must be a strong nucleophile, but also of small enough size to fit into the allowed space, and cannot be an anion. As a second consideration, it is necessary that the substituents be strongly electron-withdrawing. It is unlikely that the third NH_3 molecule would have been able to engage with the complex were it not for the strong σ-holes opposite all of the three F substituents in ZF_3.

VIII. FORCES BETWEEN IONS OF LIKE CHARGE

It is expected that under normal circumstances, a pair of ions of like charge ought to repel one another and so cannot approach close enough together to engage in a noncovalent bond. However, this idea was shown to be incorrect in the case of H-bonds where there were numerous cases of H-bonds found between a pair of cations or a pair of anions.[177–193] These counterintuitive complexes were sometimes referred to as anti-electrostatic H-bonds, and there was some exploration as to the manner in which such a H-bond can be formed. The general consensus was that within an aqueous medium, the charges of the two ions could be sufficiently dispersed by the solvent so as to allow a facile and exothermic approach even against any electrostatic repulsion. The situation in the gas phase was a bit more complicated as the complexation was found to be endothermic. The complex was thus in a metastable equilibrium, and the dissociation process encountered an energy barrier along the way. More recent work has expanded the scope of anion–anion complexation to other noncovalent bonds. Halogen bonds, too, seemed to behave in a similar way in that ions of like charge could be held together in a metastable equilibrium.[182,194–198]

Expanding the scope of such phenomena, the series of ACl_3^- anions, where A represents any of the group 2A elements Be, Mg, Ca, Sr, and Ba, was considered,[199] followed by the same bonding situation for the group 2B elements Zn, Cd, and Hg.[200] Pnicogen-bonding anions in the form of ZCl_4^- with Z = P, As, Sb were also considered[201] wherein the central atom is placed within a tetravalent bonding situation. The partner anion in each case was CN^- for purposes of consistency and to avoid complications from steric effects. The results for the entire dataset are summarized in Table XIII. The first column lists the MEP maximum of the hole $V_{s,max}$ that will be interacting with the approaching CN^-. This hole is of the π-variety above the ACl_3 plane for the groups 2A and 2B anions and a σ-hole for Group 5 ZCl_4^- that adopts a see-saw shape. Note that the value of the MEP at this maximum is highly variable, even in terms of sign. It is negative for all of the group 2B and 5A species, not conducive for the formation of a complex, particularly with another anion. The next few columns of Table XIII refer to the gas phase complexes. E_b is positive in all cases by a significant margin, so gas phase complexation is highly endothermic. Although less so, even the interaction energies are positive for the majority of these complexes. As for the HB and XB systems previously studied in the literature, these dimers are all metastable. The dissociation to the more stable pair of monomers is opposed by a substantial energy barrier $E^\dagger$ that is in the 18 kcal/mol–29 kcal/mol range.

Given the fact that the interaction of interest here occurs between a pair of anions, it is perhaps not surprising that E_b is positive, as is E_{int} with only a few exceptions. One would be tempted to surmise that these positive values are due in large part to the Coulombic repulsion. However, this presumption would be incorrect. It must be recalled that the electrostatic term is not simply equal to a charge–charge term, which of course is positive, particularly as the two monomers approach closely. A more complete evaluation of the electrostatic (ES) component of each complex listed in Table XIII shows that this term is actually negative in most cases and quite large in fact. Even when positive, ES is rather small in magnitude. So particularly, for the 2B and 5A cases, the electrostatic term is a major factor in the metastability of these complexes, tending to hold

TABLE XIII. Depth of the π-hole of monomers, and energetics of complexation with CN^- in the gas and aqueous phases, all in kcal/mol.

		Gas				aq	
	$V_{s,max}$	E_b	E_{int}	$E^{\dagger,a}$	ES	E_b	E_{int}
2A							
$BeCl_3^-$	−72.1	42.8	17.6	20.4	−6.5	−19.6	−33.1
$MgCl_3^-$	−2.0	27.7	12.4	21.9	−0.8	−15.8	−16.9
$CaCl_3^-$	+43.5	20.3	9.6	20.4	+2.1	−7.8	−8.0
$SrCl_3^-$	+34.4	19.3	8.7	17.9	+0.2	−5.5	−5.5
$BaCl_3^-$	+28.6	15.8	6.4	18.2	+3.0	−1.2	−1.2
2B							
$ZnCl_3^-$	−56.4	32.3	11.7	24.1	−41.8	−18.4	−25.8
$CdCl_3^-$	−44.8	26.9	9.3	24.1	−37.3	−12.1	−16.1
$HgCl_3^-$	−61.4	10.9	4.0	25.8	−97.0	−11.4	−20.8
5A							
PCl_4^-	−72.5	32.7	−13.1	29.1	−111.1	−22.5	−69.5
$AsCl_4^-$	−62.9	31.0	−8.7	27.0	−99.9	−23.1	−61.0
$SbCl_4^-$	−52.1	27.9	−4.2	22.8	−78.2	−22.5	−50.5

[a]Barrier to dissociation.

them together. Even for the 2A entities, ES cannot be considered as a major destabilizing factor.

The last two columns of Table XIII correspond to the situation within an aqueous medium. Because the surrounding solvent is able to disperse the charges to some extent, not only E_{int} but even E_b is negative. The complex corresponds to a fully stable structure, whose dissociation is smoothly and energetically uphill. Of the complexes considered here, it is the pnicogen-bonded dianionic systems in the last three rows that are most stably bound, both in gas and aqueous phases.

There is also recent work[202] that documents similar attractive interactions between ions as in BH_3^- or NH_3^+ homodimers or $Mn^- + CN^-$ and $Co^+ + NO^+$ pairings. Dianions, composed of course of a pair of anions, such as LiX_3^{-2}, NaX_3^{-2}, BeX_4^{-2}, and MgX_4^{-2}, also adhere to this pattern.[203]

IX. HYPERVALENT LEWIS ACIDS

Whereas most studies are concerned with Lewis acids in which the bridging atom takes on its standard valency, viz., RX, R_2Y, and R_3Z, the fact that many of these atoms occur lower in the periodic table endows them with the ability to take on more substituents, in what may be termed hypervalence. It is therefore of some importance to examine how the properties of their noncovalent bonds differ from those when in the more standard bonding patterns.

Calculations therefore considered XF_5 where a central halogen atom X was surrounded by five F substituents.[204] With one remaining lone pair on X, the geometry of this Lewis acid ought to be octahedral with the lone pair occupying one of these six positions. The chalcogen-containing YF_6 is fully octahedral with no lone pairs, but YF_4 contains a lone pair. Its geometrical framework should be a trigonal bipyramid with its lone pair at one of the three equatorial sites. With regards to hypervalent pnicogen, ZF_5 will take on a full trigonal bipyramid with no lone pairs.

The values of the σ-hole surrounding each molecule are listed in Table XIV. In the case of XF_5, the X lone pair sits directly opposite the axial F, so it displaces the σ-hole away from this position to some extent. However, even with the nearby lone pair, the σ-hole is quite positive between 45 kcal/mol and 64 kcal/mol. The NH_3 base occupies a position directly opposite the axial F, as seen in the top row of Fig. 10 for Cl, but is displaced closer to the σ-hole for X = Br and I. In any case, the binding of a base to the pentavalent XF_5 is rather strong, nearly 10 kcal/mol for Br and I and much stronger for ClF_5. Note the particularly large distortion energy for the latter.

With regard to the chalcogen systems, the congested nature of the YF_6 systems prevents a close approach of the base. In fact, it is more favorable for NH_3 to turn so as to present its H atoms and engage in NH···F H-bonds, but regardless of the nature of the bonding, it is quite weak, less than 1 kcal/mol–2 kcal/mol. The bonding is much stronger with the tetravalent YF_4 units. The σ-holes are rather intense, and the N atom can come in quite close to Y in the absence of congestion. Even stronger bonds arise in the ZF_5 systems, with E_b between 25 kcal/mol and 37 kcal/mol and E_{int} even larger. The absence of a lone pair on the central Z facilitates a strong σ-hole. It is only the large deformation energies needed to change the

TABLE XIV. Energetics of complexes of AF_n with NH_3, and σ-hole intensity, all in kcal/mol.

AF_n[a]	$V_{s,max}$	$-E_b$	$-E_{int}$
Halogen (1)			
ClF_5	45.1	16.93	46.82
BrF_5	53.6	8.56	9.42
IF_5	64.2	9.36	9.79
Chalcogen (0)			
SF_6	17.0	0.25	0.57
SeF_6	24.4	0.62	0.66
TeF_6	38.1	1.04	1.40
Chalcogen (1)			
SF_4	50.7	6.62	7.97
SeF_4	60.9	10.99	15.64
TeF_4	69.0	16.00	22.23
Pnicogen (0)			
PF_5	48.0	24.98	47.64
AsF_5	60.5	31.55	47.84
SbF_5	82.5	37.46	46.93

[a]Number of lone pairs on the central atom in parentheses.

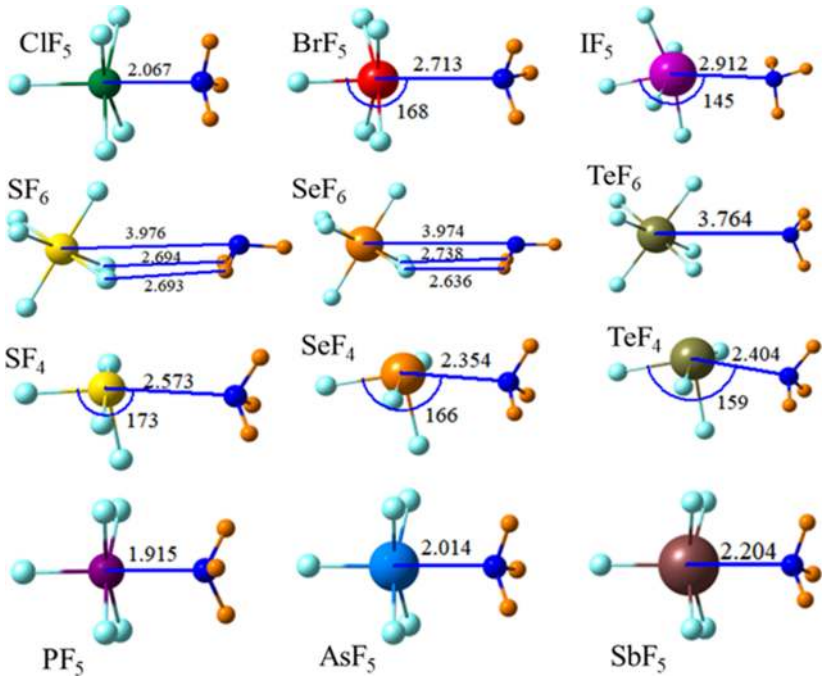

FIG. 10. Complexes formed between NH_3 and hypervalent AF_n molecules. Distances in Å and angles in degs.

internal structure of ZF_5 from a trigonal bipyramid to a square plane that keeps the binding energy from being even larger.

So, it would appear that pentavalent pnicogen atoms can engage in very strong interactions with a base, while hexavalent chalcogens are essentially unable to do so. The pentavalent halogen and tetravalent chalcogens occupy a middle ground, with noncovalent bond energies on the order of 7 kcal/mol–17 kcal/mol. This conclusion is supported by a microwave study wherein SF_6 combines with NH_3[205] to form a very weak bond, <1 kcal/mol, on which the N lone pair aligns with the C_3 axis of SF_6.

Other computations[206] show that the XB involving hypervalent halogen may be weaker than the corresponding XB involving monovalent X even when the former is more positively charged than the latter. Examination of FXO_n[207] found that the hypervalency weakens the XB, but there were multiple binding sites for the hypervalent units, some of them leading to XBs that coexist with HBs. The largest halogen At can engage in a XB with CO in its monovalent, trivalent, and pentavalent bonding environments.[208] In a comparison of BrF_3 with BrF_5, a XB to the former is linear,[209] whereas there is a certain degree of nonlinearity for the latter. SF_6 combines with NH_3[205] to form a very weak chalcogen bond, < 1 kcal/mol on which the N lone pair aligns with the C_3 axis of SF_6.

With regard to pnicogen atoms, hypervalent P in a R = PH_3 configuration[153] undergoes a reduced ^{31}P NMR chemical shielding. Pentavalent P, covalently bonded to H and F substituents,[210] generally adopts either C_{4v} or C_{2v} symmetries in its ZBs with bases and with highly variable interaction energies of as high as 46 kcal/mol. Bonding of a base to O_2ZBr[211] prefers the π-hole above the molecule in comparison to a σ-hole. When brought up to a ZOF_2X molecule,[212] a base can either form a XB with the X atom or ZB with Z; in either case, there is a good correlation between the interaction energy and maximum of the MEP. Pentavalent ZX_5[213] forms very short ZBs to pyrazine, barely longer than the sum of covalent radii. Experimental evidence has recently come to light of the ZB involving pentavalent P,[214] specifically involving $POCl_3$, and this same molecule can utilize[215] the π-electrons of an alkene, alkyne, or phenyl ring.

X. THE DITETREL BOND

One of the more interesting aspects of H-bonding is the dihydrogen bond,[110,111,216–223] which is comprised first of a typical AH acid in which the H atom is positively polarized. The molecule with which it is paired contains a MH group wherein the highly electropositive metal M atom imparts a partial negative charge to its H atom. The two molecules then come together in a AH···HM arrangement that is facilitated by the Coulombic attraction between the two H centers. Given the many similarities between the H-bond and the other noncovalent bonds discussed here, it is natural to wonder if there could be such a parallel with the dihydrogen bond as well.

Calculations considered this question in the context of a pair of tetrel atoms.[105] As pictured in Fig. 11, the Lewis acid is a standard H_3FT tetrel-containing molecule, with a F substituent so as to generate a positive σ-hole. The tetrel atom T_b on the other subunit contained a highly electron-releasing Li atom, with the goal of generating a negative region of MEP opposite the Li and toward the Lewis acid T_a.

As listed in Table XV, these substitutions produce the desired positive σ-hole on the acid and negative $V_{s,min}$ on the base T_bLiH_3. $V_{s,max}$ climbs quickly with the size of the T_a atom as expected, but $V_{s,min}$ is fairly insensitive to the nature of the T_b atom. It is a bit

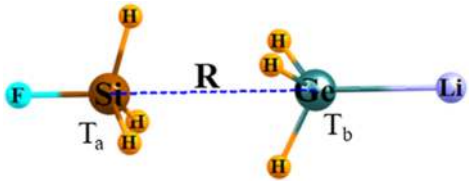

FIG. 11. Schematic diagram of the ditetrel bond, in this case between Si and Ge.

larger in magnitude for C, but the heavier T atoms have pretty much the same value. The energetics of the ditetrel bond conform nicely to these patterns in the MEP. Both E_b and E_{int} rise as T_a grows larger but have little sensitivity to T_b, outside of the aforementioned higher values for T_b=C. This systematic similarity between the energetics and MEP extrema is evident by the nearly linear red line in Fig. 12, which documents the linear dependence of the interaction energy on both $V_{s,max}$ and $V_{s,min}$. It is further interesting that the energetics are also proportional to the total charge transferred from base to acid (Q) and the stretch engendered in the F—T_a covalent bond by the formation of the ditetrel bond.

In summary, the ditetrel bond exists and is a close parallel to the dihydrogen bond. The ditetrel bond is at its strongest with C as the electron-donating atom and can be as high as 10 kcal/mol. Another parallel between the dihydrogen and ditetrel bonds is the source of the electron density coming from the base. Rather than the lone pair or π-system that is the norm, in both cases, it is one or more σ-bonding orbitals.

TABLE XV. Binding and interaction energies of ditetrel-bonded complexes, as well as the maximum of MEP of the Lewis acid monomer and MEP minimum of the base on the ρ = 0.001 a.u. isodensity surface, all in kcal/mol.

Acid	Base	$V_{s,max}$	$V_{s,min}$	$-E_b$	$-E_{int}$
FC	CLi	19.7	−39.1	2.85	2.89
FSi		37.8	−39.1	5.35	5.69
FGe		43.2	−39.1	6.35	6.84
FSn		52.9	−39.1	8.85	10.06
FPb		54.6	−39.1	9.27	10.11
FC	SiLi	19.7	−30.9	2.72	2.76
FSi		37.8	−30.9	3.88	4.01
FGe		43.2	−30.9	4.72	4.90
FSn		52.9	−30.9	6.31	6.76
FPb		54.6	−30.9	7.14	7.52
FC	GeLi	19.7	−30.6	2.73	2.76
FSi		37.8	−30.6	3.81	3.95
FGe		43.2	−30.6	4.67	4.82
FSn		52.9	−30.6	6.17	6.56
FPb		54.6	−30.6	7.06	7.40
FC	SnLi	19.7	−29.0	2.59	2.63
FSi		37.8	−29.0	3.38	3.48
FGe		43.2	−29.0	4.12	4.26
FSn		52.9	−29.0	5.35	5.70
FPb		54.6	−29.0	6.26	6.61

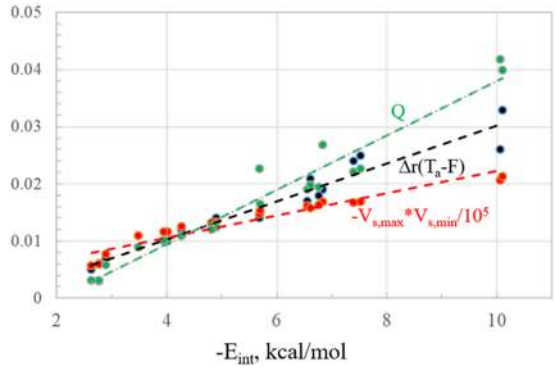

FIG. 12. Dependence on the interaction energy of the total charge transferred between molecules Q, stretch of r(T_a—F), and product of maxima and minima of the Lewis acid and base, respectively, of $H_3FT_a\cdots T_bH_3Li$ complexes.

XI. FIRST-ROW ATOMS

As mentioned earlier, the ability of an atom to serve in the capacity of the electron acceptor within the context of one of these bases is subject to both a low electronegativity and a high polarizability. For this reason, first-row atoms F, O, N, and C are not commonly observed in such bonds. Another factor is the low proclivity of these atoms to engage in hypervalent bonding, which is an implicit ingredient in these noncovalent bonds.

However, despite their handicaps, these first-row atoms do seem to participate in such bonds under certain conditions. As discussed above, the presence of electron-withdrawing substituents aids in this ability. In line with this concept, the replacement of one H atom of NH_3 by F[224] promotes its interaction with a NH_3 nucleophile in a pnicogen-bonded FN···N arrangement with a respectable interaction energy of 4 kcal/mol. Adding methyl groups to the base enhances this interaction by an additional 2 kcal/mol. Neither Cl nor Br are satisfactory in this regard as they swing around so as to engage in a halogen bond with the nucleophile. With three electron-withdrawing substituents, NF_3 is even better as an electron acceptor[225] and the NH_2F homodimer engages in a N···N ZB.[226] Calculations suggest[51] that the NH_3 base can engage in a XB with the F atom of FF or ClF. Tripathi *et al.*[227] claimed evidence of a N···N ZB in an amino acid type system. Another N···N ZB was confirmed[228] in $EtO_2N\cdots NMe_3$ by microwave spectra and calculations.

With regard to F, there are indications that F can act as an electron acceptor in certain halogen bonds. An early FT microwave study[229] suggested a XB between NH_3 and F_2. There is experimental evidence of a σ-hole on a F atom on a perfluorinated phenyl ring,[230] and the polarization of the CF_3 group in another crystal[231] suggested that there might even be F···F XBs present. Combination of crystal structural and computational data is indicative of F···F XBs.[232] There has been thought[233] that an intramolecular CF···O=C XB might lock the conformation of certain molecules. Much of the argument for the existence of a F-XB arises from crystal structure analyses where

a F atom sits in fairly close proximity to a nucleophilic atom, sometimes closer than the sum of their vdW radii. That is, a number of crystals[230,231,234–237] have shown fairly close contact of F with potential electron donor atoms, but it is not a simple matter to distinguish an interaction attractive enough to affect the structure, as opposed to one in which the atoms are placed in proximity simply because they do not repel one another. The evidence becomes a bit more convincing when the analysis of the experimentally derived electron density shows indications of a bond path. A C_6F_6 unit might be able to engage in a F···N XB with pyridine[238] but with a very shallow minimum of only 0.2 kcal/mol. This well depth was barely changed even when a number of other bases were tested.[239] Other calculations[240] are consistent with this marginally weak XB even when F is bonded to NO_2, CF_3, CN, COOH, CHO, CCH, or C≡CCF_3 substituents; the same applies to a CF_3 substituent.[234,241]

Because of its ubiquitous presence, the ability of first-row C to engage in a tetrel bond is of particular importance. There is evidence, for example, of C-tetrel bonds in various weakly bound clusters such as FCH_3 or MeOH with various bases;[242] formaldehyde with SO_2,[243] SO_3,[244] and CO_2[245] as well as CO_2 in its oligomers;[246] and interactions with various polymers,[247] amines,[248] ketones,[249] or heterocycles.[250] CO and CCN also have potential as electron acceptors.[251] It is perhaps no surprise that a methyl group can engage in a TB with an anion,[252] but its binding to an alkene or alkyne is perhaps more unexpected.[253] The density derived from x-ray data provided some evidence of a C···N TB in 1,1,2,2-tetracyano cyclopropane,[254] supported by NBO and AIM data. A combined experimental and theoretical analysis suggested a methyl TB.[255] There were also computational indications[256] of methyl participation in a TB in $XH_3C\cdots C{\equiv}NX$. An sp^2-hybridized C atom also seems capable of participating in a TB.[257] Trifluorosubstitution facilitates a C—TB in R—CF_3 groups.[258] This issue has motivated the re-examination of numerous crystal structures to probe for such bonds in both biological and chemical systems[259–265] with a particular emphasis on the C atom of methyl groups.[266–268]

Of course, one way to magnify the strength of any possible C—TB is to endow the Lewis acid with a positive charge. Calculations[269] showed that such a $CH_3^+\cdots O$ TB can reach up to 14 kcal/mol–17 kcal/mol, as compared to only 2 kcal/mol without any such charge on the acid. Such charge assistance is not limited to simply methyl groups but pertains in the case of -TF_3 as well.[270] Another avenue toward C-tetrel bonding involves deformation of a different sort. In part of a cyclopropane ring, with its intrinsic strain, a C atom in a nominal sp^3 hybridization can engage in a fairly strong TB with an O electron donor.[254,271–274] The ability is aided by the presence of a pair of highly electron-withdrawing C≡N substituents on each such C. However, this bonding is not quite of the conventional sort as it is actually the C—C midpoint between these two C atoms that is directly connected to the nucleophilic O.

A central question becomes how would one recognize a methyl TB when one is present? That is, how can one distinguish between a C···O TB and a trifurcated set of three CH···O HBs? A primary tool to make this distinction would be IR and NMR spectroscopy. Various basic groups were placed[275] near a methyl group on several Lewis acids. $S(Me)_3^+$ represents a strong Lewis acid by virtue of its overall positive charge. It was paired with NH_3, OH_2, and OCH_3^- as bases of varying strength as indicated in the top row of Fig. 13. A neutral $S(Me)_2$ is a weaker acid, but it was paired with two anions OH^- and $HCOO^-$. Finally, a tetramethylammonium cation was paired with $HCONH_2$. Altogether, these six pairs represent a wide dataset of bases interacting with a methyl group. In each set, the IR and NMR spectra were monitored as the base was moved from a clearly TB position along the R—C extension to a CH extension that would present a HB.

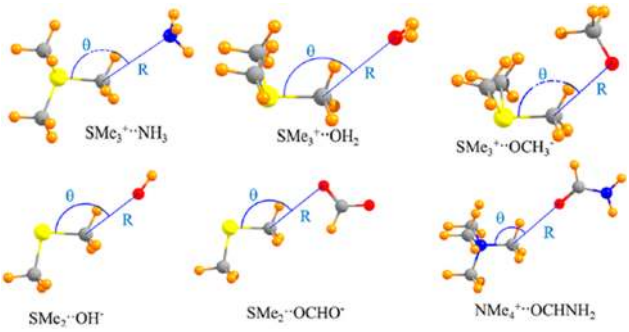

FIG. 13. Configurations of systems used to probe for the presence of the tetrel bond.

Despite the diversity of systems examined, there were several trends that appear universal.[275] As the tetrel-bonded geometry with a linear R—C···O configuration transitions to a CH···O H-bonded geometry, the methyl C—H stretching frequencies shift to the red, most notably the symmetric stretching motion. The bending frequencies move in the opposite direction, with the symmetric umbrella mode showing the largest variation. The same transition toward a HB structure produces a large downfield shift in the bridging H NMR signal, sizable enough that even the average of all three methyl H shifts ought to be measurable. The ^{13}C shielding increases on going from tetrel to H-bonded geometry, with the single exception of the $SMe_2\cdots OH^-$ complex where a rather small deshielding occurs. Of course, the magnitudes of these changes are highly dependent upon the particular system. For example, the ^{13}C shielding difference between the two configurations varies from less than 2 ppm to as much as 26 ppm for the $SMe_3^+\cdots OCH_3^-$ ion pair. Likewise, for the IR frequency changes, the umbrella bending mode change, for example, varies from a minimum of 33 cm^{-1} for $SMe_3^+\cdots OH_2$ up to as much as 128 cm^{-1} for $SMe_2\cdots OH^-$. However, the consistency of the direction of change, coupled with its large magnitude, ought to provide a framework for interpretation of the measured spectra as to the nature of the noncovalent bonding that is present.

XII. FUTURE DIRECTIONS

Work is continuing at a rapid pace to understand not only the properties of noncovalent bonds but also their influence on structure and function in chemistry and biology. One of the first orders of business appears to be a review of scores of crystal structures in order to determine whether they contain the elements of these sorts of interactions. The operational idea here is that these bonds had been hiding in plain sight for all these years. They were not noted simply because people were not looking for them. A second thrust

is the modification of extant force fields so as to accommodate these interactions. Just as special modifications were added to adjust for H-bonding interactions, so would it appear that a similar tack is needed for these H-bond cousins. One of the first steps that has been taken has been the addition of point charges to simulate the presence of σ-holes,[117,276–279] but clearly there is room for much more in this direction. Most calculations of noncovalent bonds have placed them in isolation, removed from any surroundings. It will be necessary to better understand the effects of crystal packing forces and solvation as these are the sorts of environments where these bonds typically occur. In a similar vein, experimental determination of the strengths of these bonds is urgently needed to serve as an invaluable yardstick of the accuracy of quantum calculations. On another front, spectroscopy has served as a crucial tool in identifying and characterizing H-bonds over the years. For example, the NMR chemical shift of the bridging proton and the amount of the red shift of the stretching frequency of the covalent RH bond have been widely used to estimate the H-bond strength. It is urgent to develop the same sorts of relationships and spectroscopic tools in connection with these other noncovalent bonds. It will also be interesting to monitor the gradual morphing of some of these bonds as they strengthen into what might better fit the description of covalent bonds.

DATA AVAILABILITY

The data that support the findings of this study are available from the corresponding author upon reasonable request.

REFERENCES

[1] L. R. Vieira, S. F. de Brito, M. R. Barbosa, T. O. Lopes, D. F. S. Machado, and H. C. B. de Oliveira, Phys. Chem. Chem. Phys. **22**, 17171 (2020).
[2] P. R. Herman, P. E. LaRocque, and B. P. Stoicheff, J. Chem. Phys. **89**, 4535 (1988).
[3] F. Kilchherr, C. Wachauf, B. Pelz, M. Rief, M. Zacharias, and H. Dietz, Science **353**, aaf5508 (2016).
[4] E. A. Kataev, T. A. Shumilova, B. Fiedler, T. Anacker, and J. Friedrich, J. Org. Chem. **81**, 6505 (2016).
[5] C. Trujillo and G. Sánchez-Sanz, ChemPhysChem **17**, 395 (2016).
[6] B. S. D. R. Vamhindi and A. Karton, Chem. Phys. **493**, 12 (2017).
[7] R. W. Newberry and R. T. Raines, Acc. Chem. Res. **50**, 1838 (2017).
[8] F. H. Allen, C. A. Baalham, J. P. M. Lommerse, and P. R. Raithby, Acta Crystallogr., Sect. B: Struct. Sci. **54**, 320 (1998).
[9] R. Paulini, K. Müller, and F. Diederich, Angew. Chem., Int. Ed. Engl. **44**, 1788 (2005).
[10] F. R. Fischer, P. A. Wood, F. H. Allen, and F. Diederich, Proc. Natl. Acad. Sci. U. S. A. **105**, 17290 (2008).
[11] F. W. Kotch, I. A. Guzei, and R. T. Raines, J. Am. Chem. Soc. **130**, 2952 (2008).
[12] A. Choudhary, D. Gandla, G. R. Krow, and R. T. Raines, J. Am. Chem. Soc. **131**, 7244 (2009).
[13] T. K. Pal and R. Sankararamakrishnan, J. Phys. Chem. B **114**, 1038 (2010).
[14] C. E. Jakobsche, A. Choudhary, S. J. Miller, and R. T. Raines, J. Am. Chem. Soc. **132**, 6651 (2010).
[15] S. Blanco, A. Macario, and J. C. López, Phys. Chem. Chem. Phys. **21**, 20566 (2019).
[16] H. R. Kilgore and R. T. Raines, J. Am. Chem. Soc. **140**, 17606 (2018).
[17] Y. Geboes, F. De Proft, and W. A. Herrebout, Chem. Phys. **476**, 1 (2016).
[18] M. L. DeRider, S. J. Wilkens, M. J. Waddell, L. E. Bretscher, F. Weinhold, R. T. Raines, and J. L. Markley, J. Am. Chem. Soc. **124**, 2497 (2002).
[19] K. B. Muchowska, D. J. Pascoe, S. Borsley, I. V. Smolyar, I. K. Mati, C. Adam, G. S. Nichol, K. B. Ling, and S. L. Cockroft, Angew. Chem., Int. Ed. **59**, 14602 (2020).
[20] G. C. Pimentel and A. L. McClellan, *The Hydrogen Bond* (Freeman, San Francisco, 1960).
[21] S. N. Vinogradov and R. H. Linnell, *Hydrogen Bonding* (Van Nostrand-Reinhold, New York, 1971).
[22] M. L. Huggins, Angew. Chem., Int. Ed. Engl. **10**, 147 (1971).
[23] M. D. Joesten and L. J. Schaad, *Hydrogen Bonding* (Marcel Dekker, New York, 1974).
[24] P. Schuster, G. Zundel, and C. Sandorfy, *The Hydrogen Bond: Recent Developments in Theory and Experiments* (North-Holland Publishing Co., Amsterdam, 1976).
[25] G. A. Jeffrey and W. Saenger, *Hydrogen Bonding in Biological Structures* (Springer-Verlag, Berlin, 1991).
[26] S. Scheiner, in *Pauling's Legacy: Modern Modelling of the Chemical Bond*, edited by Z. B. Maksic and W. J. Orville-Thomas (Elsevier, Amsterdam, 1997), p. 571.
[27] S. Scheiner, *Hydrogen Bonding: A Theoretical Perspective* (Oxford University Press, New York, 1997).
[28] G. Gilli and P. Gilli, *The Nature of the Hydrogen Bond* (Oxford University Press, Oxford, UK, 2009).
[29] S. Emamian, T. Lu, H. Kruse, and H. Emamian, J. Comput. Chem. **40**, 2868 (2019).
[30] A. V. Afonin and A. V. Vashchenko, Int. J. Quantum Chem. **119**, e26001 (2019).
[31] P. Su, Z. Chen, and W. Wu, Chem. Phys. Lett. **635**, 250 (2015).
[32] D. Rusinska-Roszak, J. Phys. Chem. A **119**, 3674 (2015).
[33] T. A. Hubbard, A. J. Brown, I. A. W. Bell, and S. L. Cockroft, J. Am. Chem. Soc. **138**, 15114 (2016).
[34] W. Zierkiewicz, M. Michalczyk, and S. Scheiner, Molecules **25**, 635 (2020).
[35] E. D. Stevens, Mol. Phys. **37**, 27 (1979).
[36] S. C. Nyburg and W. Wong-Ng, Proc. R. Soc. London, Ser. A **367**, 29 (1979).
[37] S. Ikuta, J. Mol. Struct.: THEOCHEM **205**, 191 (1990).
[38] J. P. M. Lommerse, A. J. Stone, R. Taylor, and F. H. Allen, J. Am. Chem. Soc. **118**, 3108 (1996).
[39] S. J. Grabowski and E. Bilewicz, Chem. Phys. Lett. **427**, 51 (2006).
[40] V. R. Hathwar and T. N. G. Row, J. Phys. Chem. A **114**, 13434 (2010).
[41] R. Sedlak, M. H. Kolář, and P. Hobza, J. Chem. Theory Comput. **11**, 4727 (2015).
[42] T. Clark, M. Hennemann, J. S. Murray, and P. Politzer, J. Mol. Model. **13**, 291 (2007).
[43] P. Politzer, J. S. Murray, and P. Lane, Int. J. Quantum Chem. **107**, 3046 (2007).
[44] A. Frontera, Molecules **25**, 3419 (2020).
[45] A. Bauzá and A. Frontera, Angew. Chem., Int. Ed. **54**, 7340 (2015).
[46] O. Hassel, Science **170**, 497 (1970).
[47] F. H. Allen, J. P. M. Lommerse, V. J. Hoy, J. A. K. Howard, and G. R. Desiraju, Acta Crystallogr., Sect. B: Struct. Sci. **53**, 1006 (1997).
[48] I. Alkorta, I. Rozas, and J. Elguero, J. Phys. Chem. A **102**, 9278 (1998).
[49] P. L. Wash, S. Ma, U. Obst, and J. Rebek, J. Am. Chem. Soc. **121**, 7973 (1999).
[50] A. C. Legon, Angew. Chem., Int. Ed. Engl. **38**, 2686 (1999).
[51] A. Karpfen, J. Phys. Chem. A **104**, 6871 (2000).
[52] P. Metrangolo and G. Resnati, Chem. - Eur. J. **7**, 2511 (2001).
[53] P. Metrangolo, H. Neukirch, T. Pilati, and G. Resnati, Acc. Chem. Res. **38**, 386 (2005).
[54] T. Caronna, R. Liantonio, T. A. Logothetis, P. Metrangolo, T. Pilati, and G. Resnati, J. Am. Chem. Soc. **126**, 4500 (2004).
[55] P. Auffinger, F. A. Hays, E. Westhof, and P. S. Ho, Proc. Natl. Acad. Sci. U. S. A. **101**, 16789 (2004).
[56] D. Swierczynski, R. Luboradzki, G. Dolgonos, J. Lipkowski, and H.-J. Schneider, Eur. J. Org. Chem. **2005**, 1172.
[57] S. Scheiner, Acc. Chem. Res. **46**, 280 (2013).
[58] K. E. Riley and K. M. Merz, J. Phys. Chem. A **111**, 1688 (2007).
[59] P. Politzer, P. Lane, M. C. Concha, Y. Ma, and J. S. Murray, J. Mol. Model. **13**, 305 (2007).

[60]A. C. Legon, Phys. Chem. Chem. Phys. **12**, 7736 (2010).
[61]R. E. Rosenfield, R. Parthasarathy, and J. D. Dunitz, J. Am. Chem. Soc. **99**, 4860 (1977).
[62]T. N. G. Row and R. Parthasarathy, J. Am. Chem. Soc. **103**, 477 (1981).
[63]G. R. Desiraju and V. Nalini, J. Mater. Chem. **1**, 201 (1991).
[64]F. T. Burling and B. M. Goldstein, J. Am. Chem. Soc. **114**, 2313 (1992).
[65]M. Iwaoka and S. Tomoda, J. Am. Chem. Soc. **118**, 8077 (1996).
[66]M. Iwaoka, S. Takemoto, and S. Tomoda, J. Am. Chem. Soc. **124**, 10613 (2002).
[67]Y. Nagao, T. Hirata, S. Goto, S. Sano, A. Kakehi, K. Iizuka, and M. Shiro, J. Am. Chem. Soc. **120**, 3104 (1998).
[68]D. B. Werz, R. Gleiter, and F. Rominger, J. Am. Chem. Soc. **124**, 10638 (2002).
[69]M. Iwaoka, H. Komatsu, T. Katsuda, and S. Tomoda, J. Am. Chem. Soc. **124**, 1902 (2002).
[70]P. Sanz, O. Mó, and M. Yáñez, Phys. Chem. Chem. Phys. **5**, 2942 (2003).
[71]C. Bleiholder, D. B. Werz, H. Köppel, and R. Gleiter, J. Am. Chem. Soc. **128**, 2666 (2006).
[72]J. S. Murray, P. Lane, T. Clark, and P. Politzer, J. Mol. Model. **13**, 1033 (2007).
[73]A. F. Cozzolino and I. Vargas-Baca, J. Organomet. Chem. **692**, 2654 (2007).
[74]K. W. Klinkhammer and P. Pyykko, Inorg. Chem. **34**, 4134 (1995).
[75]J. A. Deiters and R. R. Holmes, Phosphorus, Sulfur Silicon Relat. Elem. **123**, 329 (1997).
[76]P. Kilian, A. M. Z. Slawin, and J. D. Woollins, Chem. - Eur. J. **9**, 215 (2003).
[77]M. R. Sundberg, R. Uggla, C. Viñas, F. Teixidor, S. Paavola, and R. Kivekäs, Inorg. Chem. Commun. **10**, 713 (2007).
[78]J. Moilanen, C. Ganesamoorthy, M. S. Balakrishna, and H. M. Tuononen, Inorg. Chem. **48**, 6740 (2009).
[79]C. J. Levy and R. J. Puddephatt, J. Am. Chem. Soc. **119**, 10127 (1997).
[80]W. W. Schoeller and A. Rozhenko, Eur. J. Inorg. Chem. **2000**, 375.
[81]K. Vojinović, L. J. McLachlan, S. L. Hinchley, D. W. H. Rankin, and N. W. Mitzel, Chem. - Eur. J. **10**, 3033 (2004).
[82]A. Bauzá, T. J. Mooibroek, and A. Frontera, Angew. Chem., Int. Ed. **52**, 12317 (2013).
[83]S. J. Grabowski, Phys. Chem. Chem. Phys. **16**, 1824 (2014).
[84]S. J. Grabowski, ChemPhysChem **16**, 1470 (2015).
[85]S. Grabowski, Molecules **20**, 11297 (2015).
[86]A. Bauzá, X. García-Llinás, and A. Frontera, Chem. Phys. Lett. **666**, 73 (2016).
[87]J. Echeverría, ChemPhysChem **18**, 2864 (2017).
[88]M. Jabłoński, J. Comput. Chem. **39**, 1177 (2018).
[89]A. Bauzá and A. Frontera, Phys. Chem. Chem. Phys. **17**, 24748 (2015).
[90]E. Makarewicz, J. Lundell, A. J. Gordon, and S. Berski, J. Comput. Chem. **37**, 1876 (2016).
[91]M. D. Esrafili, S. Asadollahi, and M. Vakili, Int. J. Quantum Chem. **116**, 1254 (2016).
[92]M. Gawrilow, H. Beckers, S. Riedel, and L. Cheng, J. Phys. Chem. A **122**, 119 (2018).
[93]I. Bhattacharya, J. Sadhukhan, S. Biswas, and T. Chakraborty, J. Phys. Chem. A **124**, 7259 (2020).
[94]A. Karpfen, Comput. Theor. Chem. **1160**, 1 (2019).
[95]W. Zierkiewicz, B. Czarnik-Matusewicz, and D. Michalska, J. Phys. Chem. A **115**, 11362 (2011).
[96]N. T. Trung, T. T. Hue, and M. T. Nguyen, J. Phys. Chem. A **113**, 3245 (2009).
[97]S. Scheiner and T. Kar, J. Phys. Chem. A **106**, 1784 (2002).
[98]Y. Gu, T. Kar, and S. Scheiner, J. Am. Chem. Soc. **121**, 9411 (1999).
[99]S. Scheiner, S. J. Grabowski, and T. Kar, J. Phys. Chem. A **105**, 10607 (2001).
[100]T. Kar and S. Scheiner, J. Phys. Chem. A **108**, 9161 (2004).
[101]Y. Chen, L. Yao, and F. Wang, J. Mol. Model. **25**, 351 (2019).
[102]S. J. Grabowski and W. A. Sokalski, ChemPhysChem **18**, 1569 (2017).
[103]Y.-X. Wei, H.-B. Li, J.-B. Cheng, W.-Z. Li, and Q.-Z. Li, Int. J. Quantum Chem. **117**, e25448 (2017).
[104]S. Scheiner, T. Kar, and J. Pattanayak, J. Am. Chem. Soc. **124**, 13257 (2002).
[105]S. Scheiner, Phys. Chem. Chem. Phys. **22**, 16606 (2020).
[106]Q.-Z. Li, H.-Y. Zhuo, H.-B. Li, Z.-B. Liu, W.-Z. Li, and J.-B. Cheng, J. Phys. Chem. A **119**, 2217 (2015).
[107]S. P. Gnanasekar and E. Arunan, J. Phys. Chem. A **123**, 1168 (2019).
[108]K. Hinds, J. H. Holloway, and A. C. Legon, J. Chem. Soc., Faraday Trans. **93**, 373 (1997).
[109]I. Alkorta, J. Elguero, and J. E. Del Bene, Phys. Chem. Chem. Phys. **18**, 32593 (2016).
[110]G. Orlova and S. Scheiner, J. Phys. Chem. A **102**, 260 (1998).
[111]S. J. Grabowski and F. Ruipérez, Phys. Chem. Chem. Phys. **18**, 12810 (2016).
[112]X. Hu, H. Li, W. Liang, and S. Han, New J. Chem. **29**, 1295 (2005).
[113]T. S. Thakur and G. R. Desiraju, J. Mol. Struct.: THEOCHEM **810**, 143 (2007).
[114]S. Rizzato, J. Bergès, S. A. Mason, A. Albinati, and J. Kozelka, Angew. Chem., Int. Ed. Engl. **49**, 7440 (2010).
[115]L. R. Falvello, Angew. Chem., Int. Ed. Engl. **49**, 10045 (2010).
[116]R. Sánchez-de-Armas and M. S. G. Ahlquist, Phys. Chem. Chem. Phys. **17**, 812 (2015).
[117]M. A. A. Ibrahim, J. Mol. Model. **18**, 4625 (2012).
[118]S. Scheiner, J. Comput. Chem. **39**, 500 (2018).
[119]J. Rezac and A. de la Lande, Phys. Chem. Chem. Phys. **19**, 791 (2017).
[120]A. Forni, S. Pieraccini, S. Rendine, and M. Sironi, J. Comput. Chem. **35**, 386 (2014).
[121]H. Sun, A. Horatscheck, V. Martos, M. Bartetzko, U. Uhrig, D. Lentz, P. Schmieder, and M. Nazaré, Angew. Chem., Int. Ed. **56**, 6454 (2017).
[122]J. E. Del Bene, I. Alkorta, and J. Elguero, Theor. Chem. Acc. **133**, 1464 (2014).
[123]M. D. Esrafili, G. Mahdavinia, M. Javaheri, and H. R. Sobhi, Mol. Phys. **112**, 1161 (2014).
[124]K. E. Riley, C. L. Ford, Jr., and K. Demouchet, Chem. Phys. Lett. **621**, 165 (2015).
[125]M. D. Esrafili and F. Mohammadian-Sabet, Mol. Phys. **113**, 3559 (2015).
[126]S. J. Grabowski, Molecules **25**, 3294 (2020).
[127]H. Zhuo, H. Yu, Q. Li, W. Li, and J. Cheng, Int. J. Quantum Chem. **114**, 128 (2014).
[128]I. Alkorta, I. Soteras, J. Elguero, and J. E. Del Bene, Phys. Chem. Chem. Phys. **13**, 14026 (2011).
[129]J. E. Del Bene, I. Alkorta, and J. Elguero, J. Phys. Chem. A **120**, 5745 (2016).
[130]A. E. Reed, L. A. Curtiss, and F. Weinhold, Chem. Rev. **88**, 899 (1988).
[131]A. E. Reed, F. Weinhold, L. A. Curtiss, and D. J. Pochatko, J. Chem. Phys. **84**, 5687 (1986).
[132]B. Raghavendra and E. Arunan, Chem. Phys. Lett. **467**, 37 (2008).
[133]U. Adhikari and S. Scheiner, Chem. Phys. Lett. **532**, 31 (2012).
[134]A. J. Stone, J. Am. Chem. Soc. **135**, 7005 (2013).
[135]S. M. Huber, J. D. Scanlon, E. Jimenez-Izal, J. M. Ugalde, and I. Infante, Phys. Chem. Chem. Phys. **15**, 10350 (2013).
[136]M. Kolár, J. Hostaš, and P. Hobza, Phys. Chem. Chem. Phys. **16**, 9987 (2014).
[137]K. E. Riley, Chem. Phys. Lett. **744**, 137221 (2020).
[138]R. F. W. Bader, *Atoms in Molecules, A Quantum Theory*, International Series of Monographs in Chemistry Vol. 22 (Clarendon Press, Oxford, 1990).
[139]B. G. de Oliveira, A. Zabardasti, D. G. do Rego, and M. M. Pour, Theor. Chem. Acc. **139**, 131 (2020).
[140]S. Sarkar, M. S. Pavan, and T. N. Guru Row, Phys. Chem. Chem. Phys. **17**, 2330 (2015).
[141]Y. V. Nelyubina, A. A. Korlyukov, and K. A. Lyssenko, ChemPhysChem **16**, 676 (2015).
[142]D. Setiawan, E. Kraka, and D. Cremer, J. Phys. Chem. A **119**, 1642 (2015).
[143]J. D. Dunitz, IUCrJ **2**, 157 (2015).
[144]M. Jabłoński, J. Comput. Chem. **39**, 2183 (2018).
[145]C. R. Wick and T. Clark, J. Mol. Model. **24**, 142 (2018).
[146]S. Shahbazian, Chem. - Eur. J. **24**, 5401 (2018).
[147]M. Solimannejad, E. Bayati, and M. D. Esrafili, Mol. Phys. **112**, 2058 (2014).
[148]M. Jablonski and M. Palusiak, Chem. Phys. **415**, 207 (2013).
[149]M. Jablonski, J. Phys. Chem. A **116**, 3753 (2012).

[150]Z. A. Keyvani, S. Shahbazian, and M. Zahedi, Chem. - Eur. J. **22**, 5003 (2016).
[151]D. Myburgh, S. von Berg, and J. Dillen, J. Comput. Chem. **39**, 2273 (2018).
[152]E. C. Escudero-Adán, A. Bauzá, C. Lecomte, A. Frontera, and P. Ballester, Phys. Chem. Chem. Phys. **20**, 24192 (2018).
[153]I. Alkorta, G. Sánchez-Sanz, J. Elguero, and J. E. Del Bene, J. Phys. Chem. A **118**, 1527 (2014).
[154]I. Alkorta, I. Rozas, and J. Elguero, J. Phys. Chem. A **105**, 743 (2001).
[155]D. Kaur, R. Kaur, and B. A. Shiekh, Struct. Chem. **27**, 961 (2016).
[156]T. L. Ellington, P. L. Reves, B. L. Simms, J. L. Wilson, D. L. Watkins, G. S. Tschumper, and N. I. Hammer, ChemPhysChem **18**, 1267 (2017).
[157]H. Torii, Phys. Chem. Chem. Phys. **21**, 17118 (2019).
[158]I. Alkorta, M. M. Montero-Campillo, O. Mó, J. Elguero, and M. Yáñez, J. Phys. Chem. A **123**, 7124 (2019).
[159]V. Kumar, Y. Xu, C. Leroy, and D. L. Bryce, Phys. Chem. Chem. Phys. **22**, 3817 (2020).
[160]Y. Tao, Y. Qiu, W. Zou, S. Nanayakkara, S. Yannacone, and E. Kraka, Molecules **25**, 1589 (2020).
[161]W. Wang and P. Hobza, J. Phys. Chem. A **112**, 4114 (2008).
[162]W. Wang, Y. Zhang, and B. Ji, J. Phys. Chem. A **114**, 7257 (2010).
[163]D. Hauchecorne, A. Moiana, B. J. van der Veken, and W. A. Herrebout, Phys. Chem. Chem. Phys. **13**, 10204 (2011).
[164]Y.-S. Wang, C.-C. Yin, and S. D. Chao, J. Chem. Phys. **141**, 134308 (2014).
[165]A. Karpfen and E. S. Kryachko, J. Phys. Chem. A **113**, 5217 (2009).
[166]R. L. T. Parreira, S. E. Galembeck, and P. Hobza, ChemPhysChem **8**, 87 (2007).
[167]A. Mukhopadhyay, M. Mukherjee, P. Pandey, A. K. Samanta, R. Bandyopadhyay, and T. Chakraborty, J. Phys. Chem. A **113**, 3078 (2008).
[168]P. R. Shirhatti and S. Wategaonkar, Phys. Chem. Chem. Phys. **12**, 6650 (2010).
[169]W. Wang, N.-B. Wong, W. Zheng, and A. Tian, J. Phys. Chem. A **108**, 1799 (2004).
[170]S. J. Grabowski, Phys. Chem. Chem. Phys. **19**, 29742 (2017).
[171]E. Solel and S. Kozuch, Molecules **23**, 2742 (2018).
[172]S. Scheiner, J. Phys. Chem. A **121**, 5561 (2017).
[173]R. Wysokiński, M. Michalczyk, W. Zierkiewicz, and S. Scheiner, Phys. Chem. Chem. Phys. **21**, 10336 (2019).
[174]W. Zierkiewicz, M. Michalczyk, R. Wysokiński, and S. Scheiner, Molecules **24**, 376 (2019).
[175]W. Zierkiewicz, R. Wysokiński, M. Michalczyk, and S. Scheiner, Phys. Chem. Chem. Phys. **21**, 20829 (2019).
[176]R. Wysokiński, W. Zierkiewicz, M. Michalczyk, and S. Scheiner, J. Phys. Chem. A **124**, 2046 (2020).
[177]S. R. Kass, J. Am. Chem. Soc. **127**, 13098 (2005).
[178]A. Shokri, M. Ramezani, A. Fattahi, and S. R. Kass, J. Phys. Chem. A **117**, 9252 (2013).
[179]F. Weinhold and R. A. Klein, Angew. Chem., Int. Ed. **53**, 11214 (2014).
[180]I. Mata, E. Molins, I. Alkorta, and E. Espinosa, J. Phys. Chem. A **119**, 183 (2014).
[181]M. Vazdar, J. Vymetal, J. Heyda, J. Vondrasek, and P. Jungwirth, J. Phys. Chem. A **115**, 11193 (2011).
[182]C. Wang, Y. Fu, L. Zhang, D. Danovich, S. Shaik, and Y. Mo, J. Comput. Chem. **39**, 481 (2018).
[183]Y. Yang, Z. Xu, Z. Zhang, Z. Yang, Y. Liu, J. Wang, T. Cai, S. Li, K. Chen, J. Shi, and W. Zhu, J. Phys. Chem. B **119**, 11988 (2015).
[184]I. Alkorta, I. Mata, E. Molins, and E. Espinosa, Chem. - Eur. J. **22**, 9226 (2016).
[185]E. M. Fatila, E. B. Twum, A. Sengupta, M. Pink, J. A. Karty, K. Raghavachari, and A. H. Flood, Angew. Chem., Int. Ed. **55**, 14057 (2016).
[186]R. Prohens, A. Portell, M. Font-Bardia, A. Bauzá, and A. Frontera, Chem. Commun. **54**, 1841 (2018).
[187]F. Weinhold, Inorg. Chem. **57**, 2035 (2018).
[188]R. Barbas, R. Prohens, A. Bauzá, A. Franconetti, and A. Frontera, Chem. Commun. **55**, 115 (2019).
[189]Í. Iribarren, M. M. Montero-Campillo, I. Alkorta, J. Elguero, and D. Quiñonero, Phys. Chem. Chem. Phys. **21**, 5796 (2019).
[190]T. Niemann, P. Stange, A. Strate, and R. Ludwig, Phys. Chem. Chem. Phys. **21**, 8215 (2019).
[191]S. G. Dash and T. S. Thakur, Phys. Chem. Chem. Phys. **21**, 20647 (2019).
[192]N. G. White, CrystEngComm **21**, 4855 (2019).
[193]L. M. Azofra, J. Elguero, and I. Alkorta, J. Phys. Chem. A **124**, 2207 (2020).
[194]D. Quiñonero, I. Alkorta, and J. Elguero, Phys. Chem. Chem. Phys. **18**, 27939 (2016).
[195]G. Wang, Z. Chen, Z. Xu, J. Wang, Y. Yang, T. Cai, J. Shi, and W. Zhu, J. Phys. Chem. B **120**, 610 (2016).
[196]S. M. Chalanchi, I. Alkorta, J. Elguero, and D. Quiñonero, ChemPhysChem **18**, 3462 (2017).
[197]Z. Zhu, G. Wang, Z. Xu, Z. Chen, J. Wang, J. Shi, and W. Zhu, Phys. Chem. Chem. Phys. **21**, 15106 (2019).
[198]J. M. Holthoff, E. Engelage, R. Weiss, and S. M. Huber, Angew. Chem., Int. Ed. **59**, 11150 (2020).
[199]W. Zierkiewicz, R. Wysokiński, M. Michalczyk, and S. Scheiner, ChemPhysChem **21**, 870 (2020).
[200]R. Wysokiński, W. Zierkiewicz, M. Michalczyk, and S. Scheiner, ChemPhysChem **21**, 1119 (2020).
[201]S. Scheiner, R. Wysokiński, M. Michalczyk, and W. Zierkiewicz, J. Phys. Chem. A **124**, 4998 (2020).
[202]F. Weinhold, Angew. Chem., Int. Ed. **56**, 14577 (2017).
[203]D. Quiñonero, I. Alkorta, and J. Elguero, ChemPhysChem **21**, 1597 (2020).
[204]S. Scheiner and J. Lu, Chem. - Eur. J. **24**, 8167 (2018).
[205]D. M. Bittner, D. P. Zaleski, S. L. Stephens, N. R. Walker, and A. C. Legon, ChemPhysChem **16**, 2630 (2015).
[206]W. Wang, J. Phys. Chem. A **115**, 9294 (2011).
[207]N. Cheng, F. Bi, Y. Liu, C. Zhang, and C. Liu, New J. Chem. **38**, 1256 (2014).
[208]F. Zhou, Y. Liu, Z. Wang, T. Lu, Q. Yang, Y. Liu, and B. Zheng, Phys. Chem. Chem. Phys. **21**, 15310 (2019).
[209]S. J. Grabowski, Chem. Phys. Lett. **605-606**, 131 (2014).
[210]J. E. Del Bene, I. Alkorta, and J. Elguero, J. Phys. Chem. A **118**, 10144 (2014).
[211]A. Bauzá, R. Ramis, and A. Frontera, J. Phys. Chem. A **118**, 2827 (2014).
[212]M. D. Esrafili and N. Mohammadirad, Struct. Chem. **27**, 939 (2016).
[213]J. Fanfrlík, W. Zierkiewicz, P. Švec, Z. Růžičková, J. Řezáč, M. Michalczyk, A. Růžička, D. Michalska, and P. Hobza, J. Mol. Model. **23**, 328 (2017).
[214]P. K. Sruthi, N. Ramanathan, S. Sarkar, and K. Sundararajan, Phys. Chem. Chem. Phys. **20**, 22058 (2018).
[215]P. K. Sruthi, S. Sarkar, N. Ramanathan, and K. Sundararajan, Phys. Chem. Chem. Phys. **21**, 12250 (2019).
[216]R. Custelcean and J. E. Jackson, Chem. Rev. **101**, 1963 (2001).
[217]D. J. Ingram, T. F. Headen, N. T. Skipper, S. K. Callear, M. Billing, and A. Sella, Phys. Chem. Chem. Phys. **20**, 12200 (2018).
[218]J. Fanfrlík, J. Holub, Z. Růžičková, J. Řezáč, P. D. Lane, D. A. Wann, D. Hnyk, A. Růžička, and P. Hobza, ChemPhysChem **17**, 3373 (2016).
[219]S. J. Grabowski, J. Phys. Org. Chem. **26**, 452 (2013).
[220]B. G. d. Oliveira, Phys. Chem. Chem. Phys. **15**, 37 (2013).
[221]T. Kar and S. Scheiner, J. Chem. Phys. **119**, 1473 (2003).
[222]M. Solimannejad and S. Scheiner, J. Phys. Chem. A **109**, 11933 (2005).
[223]H. Cybulski, E. Tymińska, and J. Sadlej, ChemPhysChem **7**, 629 (2006).
[224]S. Scheiner, Chem. Phys. Lett. **514**, 32 (2011).
[225]F. Blanco, I. Alkorta, I. Rozas, M. Solimannejad, and J. Elguero, Phys. Chem. Chem. Phys. **13**, 674 (2011).
[226]I. Alkorta, G. Sánchez-Sanz, J. Elguero, and J. E. Del Bene, J. Phys. Chem. A **117**, 183 (2013).
[227]G. Tripathi, K. Badi-uz-zama, and G. Ramanathan, Chem. Phys. Lett. **653**, 117 (2016).
[228]W. Li, L. Spada, N. Tasinato, S. Rampino, L. Evangelisti, A. Gualandi, P. G. Cozzi, S. Melandri, V. Barone, and C. Puzzarini, Angew. Chem., Int. Ed. **57**, 13853 (2018).

[229]H. I. Bloemink, K. Hinds, J. H. Holloway, and A. C. Legon, Chem. Phys. Lett. **245**, 598 (1995).
[230]M. S. Pavan, K. Durga Prasad, and T. N. Guru Row, Chem. Commun. **49**, 7558 (2013).
[231]V. R. Hathwar, D. Chopra, P. Panini, and T. N. Guru Row, Cryst. Growth Des. **14**, 5366 (2014).
[232]R. M. Osuna, V. Hernández, J. T. L. Navarrete, E. D'Oria, and J. J. Novoa, Theor. Chem. Acc. **128**, 541 (2011).
[233]D. Dey, S. Bhandary, A. Sirohiwal, V. R. Hathwar, and D. Chopra, Chem. Commun. **52**, 7225 (2016).
[234]P. Metrangolo, J. S. Murray, T. Pilati, P. Politzer, G. Resnati, and G. Terraneo, Cryst. Growth Des. **11**, 4238 (2011).
[235]A. G. Dikundwar and T. N. G. Row, Cryst. Growth Des. **12**, 1713 (2012).
[236]A. Sirohiwal, V. R. Hathwar, D. Dey, R. Regunathan, and D. Chopra, Acta Crystallogr., Sect. B: Struct. Sci., Cryst. Eng. Mater. **73**, 140 (2017).
[237]C. Jelsch and B. Guillot, Acta Crystallogr., Sect. B: Struct. Sci., Cryst. Eng. Mater. **73**, 136 (2017).
[238]S. Tsuzuki, A. Wakisaka, T. Ono, and T. Sonoda, Chem. - Eur. J. **18**, 951 (2012).
[239]A. Varadwaj, P. R. Varadwaj, and B.-Y. Jin, RSC Adv. **6**, 19098 (2016).
[240]Y. Wang, J. Tong, W. Wu, Z. Xu, and Y. Lu, Int. J. Quantum Chem. **115**, 884 (2015).
[241]A. Varadwaj, P. R. Varadwaj, and B.-Y. Jin, Int. J. Quantum Chem. **115**, 453 (2015).
[242]D. Mani and E. Arunan, Phys. Chem. Chem. Phys. **15**, 14377 (2013).
[243]L. M. Azofra and S. Scheiner, J. Chem. Phys. **140**, 034302 (2014).
[244]L. M. Azofra, I. Alkorta, and S. Scheiner, Phys. Chem. Chem. Phys. **16**, 18974 (2014).
[245]L. M. Azofra and S. Scheiner, J. Chem. Phys. **142**, 034307 (2015).
[246]L. M. Azofra and S. Scheiner, Phys. Chem. Chem. Phys. **16**, 5142 (2014).
[247]S. G. Kazarian, M. F. Vincent, F. V. Bright, C. L. Liotta, and C. A. Eckert, J. Am. Chem. Soc. **118**, 1729 (1996).
[248]T. Lu, J. Zhang, Q. Gou, and G. Feng, Phys. Chem. Chem. Phys. **22**, 8467 (2020).
[249]M. Li, J. Lei, G. Feng, J.-U. Grabow, and Q. Gou, Spectrochim. Acta, Part A **238**, 118424 (2020).
[250]I. Alkorta, J. Elguero, and J. E. Del Bene, J. Phys. Chem. A **121**, 8017 (2017).
[251]I. Alkorta, F. Blanco, J. Elguero, J. A. Dobado, S. M. Ferrer, and I. Vidal, J. Phys. Chem. A **113**, 8387 (2009).
[252]A. Bauzá, T. J. Mooibroek, and A. Frontera, Chem. Commun. **50**, 12626 (2014).
[253]D. Mani and E. Arunan, J. Phys. Chem. A **118**, 10081 (2014).
[254]E. C. Escudero-Adán, A. Bauzá, A. Frontera, and P. Ballester, ChemPhysChem **16**, 2530 (2015).
[255]P. Pal, S. Konar, P. Lama, K. Das, A. Bauzá, A. Frontera, and S. Mukhopadhyay, J. Phys. Chem. B **120**, 6803 (2016).
[256]M. D. Esrafili, H. Kiani, and F. Mohammadian-Sabet, Mol. Phys. **114**, 3658 (2016).
[257]D. Quiñonero, Phys. Chem. Chem. Phys. **19**, 15530 (2017).
[258]X. García-Llinás, A. Bauzá, S. K. Seth, and A. Frontera, J. Phys. Chem. A **121**, 5371 (2017).
[259]S. A. Southern and D. L. Bryce, J. Phys. Chem. A **119**, 11891 (2015).
[260]A. Bauzá and A. Frontera, Cryst **6**, 26 (2016).
[261]C. Packianathan, P. Kandavelu, and B. P. Rosen, Biochem **57**, 4083 (2018).
[262]A. Gholipour, Struct. Chem. **29**, 1255 (2018).
[263]V. R. Mundlapati, D. K. Sahoo, S. Bhaumik, S. Jena, A. Chandrakar, and H. S. Biswal, Angew. Chem., Int. Ed. **57**, 16496 (2018).
[264]T. J. Mooibroek, Molecules **24**, 3370 (2019).
[265]A. Daolio, P. Scilabra, G. Terraneo, and G. Resnati, Coord. Chem. Rev. **413**, 213265 (2020).
[266]R. C. Trievel and S. Scheiner, Molecules **23**, 2965 (2018).
[267]S. P. Thomas, M. S. Pavan, and T. N. Guru Row, Chem. Commun. **50**, 49 (2014).
[268]E. Bartashevich, Y. Matveychuk, and V. Tsirelson, Molecules **24**, 1083 (2019).
[269]S. Scheiner, J. Phys. Chem. A **119**, 9189 (2015).
[270]M. Liu, Q. Li, and S. Scheiner, Phys. Chem. Chem. Phys. **19**, 5550 (2017).
[271]J. J. Roeleveld, S. J. Lekanne Deprez, A. Verhoofstad, A. Frontera, J. I. van der Vlugt, and T. J. Mooibroek, Chem. - Eur. J. **26**, 10126 (2020).
[272]A. Bauzá, A. Frontera, and T. J. Mooibroek, Phys. Chem. Chem. Phys. **18**, 1693 (2016).
[273]V. L. Heywood, T. P. J. Alford, J. J. Roeleveld, S. J. Lekanne Deprez, A. Verhoofstad, J. I. van der Vlugt, S. R. Domingos, M. Schnell, A. P. Davis, and T. J. Mooibroek, Chem. Sci. **11**, 5289 (2020).
[274]A. Bauzá, T. J. Mooibroek, and A. Frontera, Chem. - Eur. J. **20**, 10245 (2014).
[275]S. Scheiner, J. Phys. Chem. A **122**, 7852 (2018).
[276]M. Campetella, N. De Mitri, and G. Prampolini, J. Chem. Phys. **153**, 044106 (2020).
[277]D. Franchini, F. Dapiaggi, S. Pieraccini, A. Forni, and M. Sironi, Chem. Phys. Lett. **712**, 89 (2018).
[278]R. Nunes, D. Vila-Viçosa, M. Machuqueiro, and P. J. Costa, J. Chem. Theory Comput. **14**, 5383 (2018).
[279]M. Kolár, P. Hobza, and A. K. Bronowska, Chem. Commun. **49**, 981 (2013).